iScience

CellPress

Article

Endocannabinoid LTD in Accumbal D1 Neurons Mediates Reward-Seeking Behavior

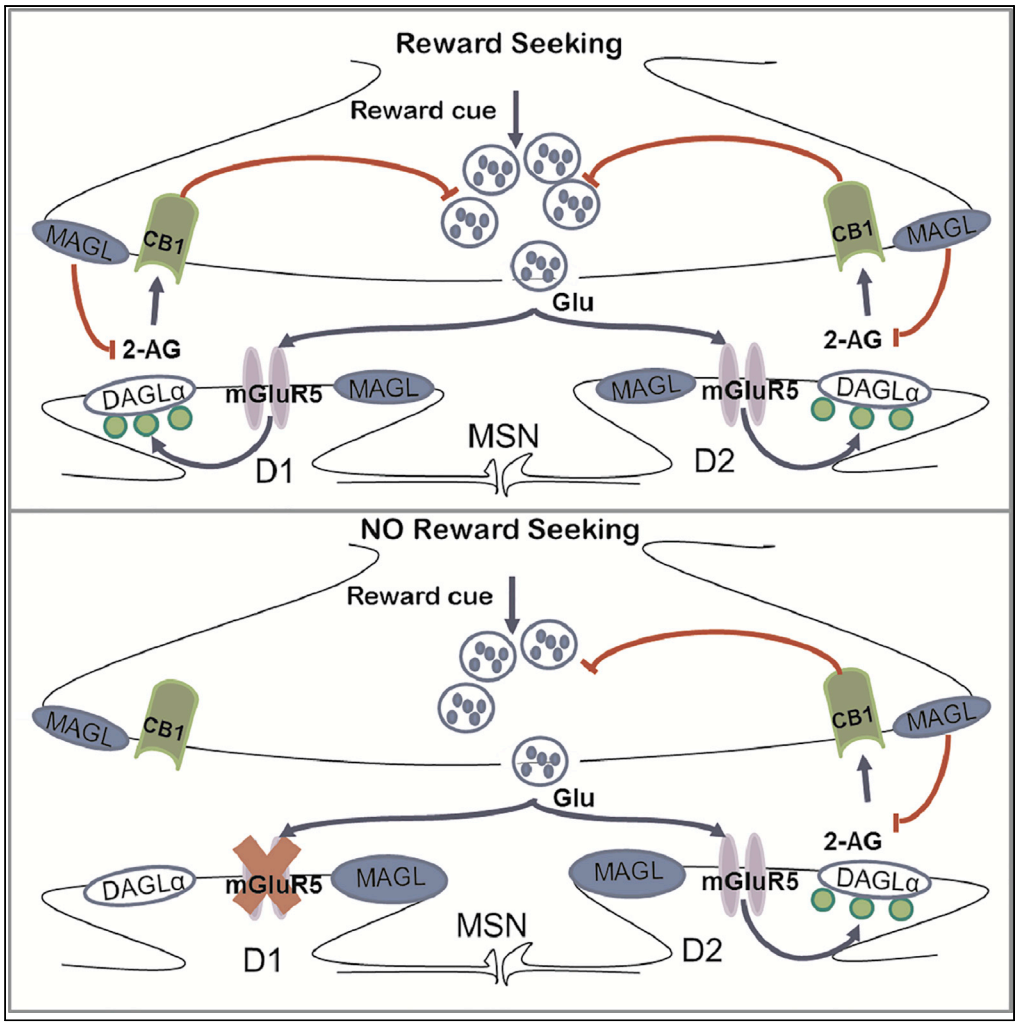

Ainhoa Bilbao, Daniela Neuhofer, Marja Sepers, ..., Beat Lutz, Olivier J. Manzoni, Rainer Spanagel

ainhoa.bilbao@zi-mannheim.de (A.B.)
olivier.manzoni@inserm.fr (O.J.M.)
rainer.spanagel@zi-mannheim.de (R.S.)

HIGHLIGHTS

mGluR5-D1-CB1-induced eCB-LTD mediates drugs of abuse and natural reward seeking

eCB-LTD in D2-MSNs plays no important role in processing of reward-seeking responses

Loss of eCB-LTD is a consequence of higher MAGL activity and lower CB1R expression

Acute drug administration stops craving for alternative rewards on following days

Bilbao et al., iScience *23*, 100951
March 27, 2020
https://doi.org/10.1016/j.isci.2020.100951

iScience

CellPress

Article

Endocannabinoid LTD in Accumbal D1 Neurons Mediates Reward-Seeking Behavior

Ainhoa Bilbao,[1,2,10,*] Daniela Neuhofer,[3,4] Marja Sepers,[3,4] Shou-peng Wei,[1,2] Manuela Eisenhardt,[1,2] Sarah Hertle,[1,2] Olivier Lassalle,[3,4,5] Almudena Ramos-Uriarte,[6,7] Nagore Puente,[6,7] Raissa Lerner,[8] Pedro Grandes,[6,7] Beat Lutz,[8] Olivier J. Manzoni,[3,4,5,9,*] and Rainer Spanagel[2,9,*]

SUMMARY

The nucleus accumbens (NAc) plays a key role in drug-related behavior and natural reward learning. Synaptic plasticity in dopamine D1 and D2 receptor medium spiny neurons (MSNs) of the NAc and the endogenous cannabinoid (eCB) system have been implicated in reward seeking. However, the precise molecular and physiological basis of reward-seeking behavior remains unknown. We found that the specific deletion of metabotropic glutamate receptor 5 (mGluR5) in D1-expressing MSNs ($D1^{miR}$mGluR5 mice) abolishes eCB-mediated long-term depression (LTD) and prevents the expression of drug (cocaine and ethanol), natural reward (saccharin), and brain-stimulation-seeking behavior. *In vivo* enhancement of 2-arachidonoylglycerol (2-AG) eCB signaling within the NAc core restores both eCB-LTD and reward-seeking behavior in $D1^{miR}$mGluR5 mice. The data suggest a model where the eCB and glutamatergic systems of the NAc act in concert to mediate reward-seeking responses.

INTRODUCTION

The brain reward system mediates motivational responses to natural rewards such as drinking, eating, and reproduction. Reinforcement learning for natural rewards depends on the formation of long-lasting conditioned associations that result in reward-seeking responses. This form of learning involves synaptic plasticity within the reward system, notably in medium spiny neurons (MSNs) of the nucleus accumbens (NAc) (Russo et al., 2010; Lüscher and Malenka, 2011). Drugs of abuse also act through the reward system, but the extent to which drug rewards and natural rewards share common neurobiological mechanisms within the reward system is barely studied.

One mechanism by which drugs of abuse alter synaptic plasticity in the reward system involves endocannabinoids (eCB). Stimulation of prelimbic cortex afferents at naturally occurring frequencies can cause long-term depression (LTD) of NAc glutamatergic synapses—an effect mediated by eCB release and presynaptic cannabinoid type 1receptor (CB1R) (Robbe et al., 2002; Zlebnik and Cheer, 2016; Araque et al., 2017). This form of eCB-mediated synaptic plasticity in the NAc depends on postsynaptic metabotropic glutamate receptor 5 (mGluR5) and is eliminated following exposure to drugs of abuse (Mato et al., 2004; Fourgeaud et al., 2004; Zlebnik and Cheer, 2016).

Although a direct involvement of this particular form of plasticity in reinforcement learning has so far not been demonstrated, there is increasing evidence that both mGluR5 and CB1R are critical for the expression of eCB-induced LTD and are involved in reward-seeking responses. Thus systemic pharmacological blockade of mGluR5 (Bäckström et al., 2004; Olive, 2009; Wang et al., 2013; Mihov and Hasler, 2016) or CB1R (De Vries et al., 2001; Cippitelli et al., 2005) reduces cue-induced reinstatement of drug-seeking responses. mGluR5 blockade also increases intracranial self-stimulation (ICSS) thresholds, suggesting a deficit in brain reward function (Cleva et al., 2012). The anatomical loci and neuronal mechanisms underlying these effects of CB1R and mGluR5 antagonists are still not well defined, but a specific role of CB1R in the NAc has been demonstrated for cocaine-, heroin-, and nicotine-seeking behavior in rodents (Xi et al., 2006; Kodas et al., 2007; Alvarez-Jaimes et al., 2008). Likewise mGluR5 in the NAc is also critically involved in drug-seeking behavior. Thus genetic deletion of mGluR5 in the NAc (Novak et al., 2010), intra-NAc administration of a selective mGluR5 antagonist (Knackstedt et al., 2014), and pharmacological inhibition of mGluR5 signaling via Homer proteins reduce cue-induced cocaine-seeking (Wang et al., 2013). Furthermore, combining sub-threshold doses of mGlu5R and CB1R antagonists also prevents alcohol-seeking behavior (Adams et al., 2010), suggesting an interaction between these two systems in mediating

[1]Behavioral Genetics Research Group, Heidelberg University, Medical Faculty Mannheim, 68159 Mannheim, Germany

[2]Institute of Psychopharmacology, Central Institute of Mental Health, Heidelberg University, Medical Faculty Mannheim, 68159 Mannheim, Germany

[3]INSERM U1249, Parc Scientifique de Luminy - BP 13 - 13273, Marseille Cedex 09, France

[4]Aix-Marseille University, Jardindu Pharo, 58 Boulevard Charles Livon, Marseille, 13007, France

[5]Cannalab, Cannabinoids Neuroscience Research International Associated Laboratory, INSERM-Indiana University, 107 S Indiana Avenue, Bloomington, IN 47405, USA

[6]Department of Neurosciences, Faculty of Medicine and Nursing, University of the Basque Country UPV/EHU, Barrio Sarriena s/n, 48940 Leioa, Spain

[7]Achucarro Basque Center for Neuroscience, Science Park of the UPV/EHU, Barrio Sarriena s/n, 48940 Leioa, Spain

[8]Institute of Physiological Chemistry, University Medical Center of the Johannes Gutenberg, University Mainz, Duesbergweg 6, 55099 Mainz, Germany

[9]These authors contributed equally

[10]Lead Contact

*Correspondence: ainhoa.bilbao@zi-mannheim.de (A.B.), olivier.manzoni@inserm.fr (O.J.M.), rainer.spanagel@zi-mannheim.de (R.S.)

https://doi.org/10.1016/j.isci.2020.100951

drug-seeking behavior. mGluR5 and CB1R blockade may also reduce seeking for food and other natural rewards. However, these findings are less consistent compared with those using drug rewards (Fattore et al., 2007; Sanchis-Segura et al., 2004; Olive, 2009; Sinclair et al., 2012; Watterson et al., 2013; Schmidt et al., 2015; Mihov and Hasler, 2016).

Two fundamental but unresolved issues are whether eCB-mediated synaptic plasticity that depends on presynaptic CB1R and postsynaptic mGluR5 in the NAc is causally involved in drug-seeking responses and whether the extent to which these synaptic changes also mediate natural reward-seeking responses; i.e., is there a common or distinct synaptic mechanism involved in drug and natural reward-seeking behavior. Here we mainly focused on e-CB-mediated synaptic plasticity in dopamine D1-receptor-containing MSNs, as several studies (Calipari et al., 2016; Hikida et al., 2010; Lobo and Nestler, 2011; Ma et al., 2018; Soares-Cunha et al., 2016) suggest that this neuronal population seems to be more likely involved in the formation of drug/natural reward-seeking behavior than D2-containing MSNs.

RESULTS

mGluR5 in D1-Containing Neurons Mediate Drug- and Natural Reward-Seeking Behavior

Using a conditional mouse model with a knockdown of mGluR5 in dopamine D1-receptor-containing neurons ($D1^{miR}$mGluR5 mice), we recently demonstrated that mGluR5 in this specific neuronal population mediates cue-induced reinstatement of cocaine-seeking behavior (Novak et al., 2010). Using this mouse model, we further asked if reward-seeking responses toward other drugs of abuse and natural rewards are also affected by this selective deletion of mGluR5 in D1-containing neurons. We first assessed ethanol-seeking responses in the reinstatement paradigm. $D1^{miR}$mGluR5 mutants and wild-type littermates were trained under operant conditions. According to our standard protocol (Eisenhardt et al., 2015) mice were then trained for 15 days in 30-min sessions to lever press for ethanol with the presentation of contextual cues (S^+/CS^+) predictive of ethanol availability. All mice acquired stable lever pressing for ethanol (Figure S1A, two-way ANOVA, *genotype* effect: $F_{(1,22)} = 0.3$, $p = 0.6$; *genotype* × *time* interaction: $F_{(14,308)} = 1.2$, $p = 0.3$). Likewise, no genotype difference was observed during a 15-day extinction phase (Figure S1B, two-way ANOVA, *genotype* effect: $F_{(1,22)} = 0.2$, $p = 0.7$; *session* effect: $F_{(14,308)} = 9.3$, $p < 0.0001$). One day after the last extinction session, mice were tested for cue-induced reinstatement of ethanol seeking. The presentation of S^+/CS^+ significantly reinstated ethanol-seeking behavior in wild-type mice—an effect that was absent in mutant mice (Figure 1A left, two-way ANOVA, *genotype*: $F_{(1,22)} = 6.1$, $p < 0.05$, *cue* $F_{(2,44)} = 41.6$, $p < 0.0001$, and a *cue* × *genotype* interaction effect: $F_{(2,44)} = 5.5$, $p < 0.01$). These findings extend our previous observation of a similar phenotype with cocaine-associated cues (Novak et al., 2010) and demonstrate that mGluR5 in D1 neurons is a mediator of drug/cue memories and drug-seeking responses.

We next examined whether mGluR5 in D1 neurons is involved in the general processing of conditioned reward-seeking responses. For this purpose, a second group of mice was tested for its seeking behavior toward saccharin, a natural reward. During acquisition and extinction phases, again no genotype differences were observed for saccharin responding (Figure S1B and S1C two-way ANOVA, *genotype* effect: $F_{(1,27)} = 0.8$, $p = 0.8$ for acquisition and *genotype* effect: $F_{(1,27)} = 2.2$, $p = 0.1$ for extinction). Presentation of the S^+/CS^+ stimuli triggered reinstatement of saccharin-seeking behavior in wild-type mice but not in $D1^{miR}$mGluR5 mice (Figure 1B left, two-way ANOVA, *genotype*: $F_{(1,27)} = 10.7$, $p < 0.005$, *cue* $F_{(2,54)} = 40.6$, $p < 0.0001$, and a *cue* × *genotype* interaction effect: $F_{(2,54)} = 7.5$, $p < 0.005$) demonstrating that mGluR5 in D1 neurons is also critical for natural reward-seeking responses.

Systemic administration of mGluR5 antagonists also reduces drug-seeking responses as well as saccharin-seeking responses (Bäckström et al., 2004; Olive, 2009; Watterson et al., 2013; Mihov and Hasler, 2016). If mGluR5 in D1-containing neurons would solely contribute to this systemic drug effect, reward-seeking responses in $D1^{miR}$mGluR5 mice should not further be affected by mGluR5 antagonist. Therefore, we studied the effects of 2-methyl-6-(phenylethynyl)pyridine (MTEP 20 mg/kg) on cue-induced reinstatement of ethanol and saccharin seeking in our mutant mice. As expected, in comparison to vehicle, MTEP reduced the reinstatement response for ethanol-seeking behavior and saccharin-seeking behavior in wild-type mice. However, MTEP had no further effect in $D1^{miR}$mGluR5 mice on the already reduced reinstatement (Figure 1A right, two-way ANOVA, *treatment* effect $F_{(1,10)} = 6.7$; $p < 0.05$ and Figure 1B right, *treatment* effect $F_{(1,27)} = 48.6$; $p < 0.0001$).

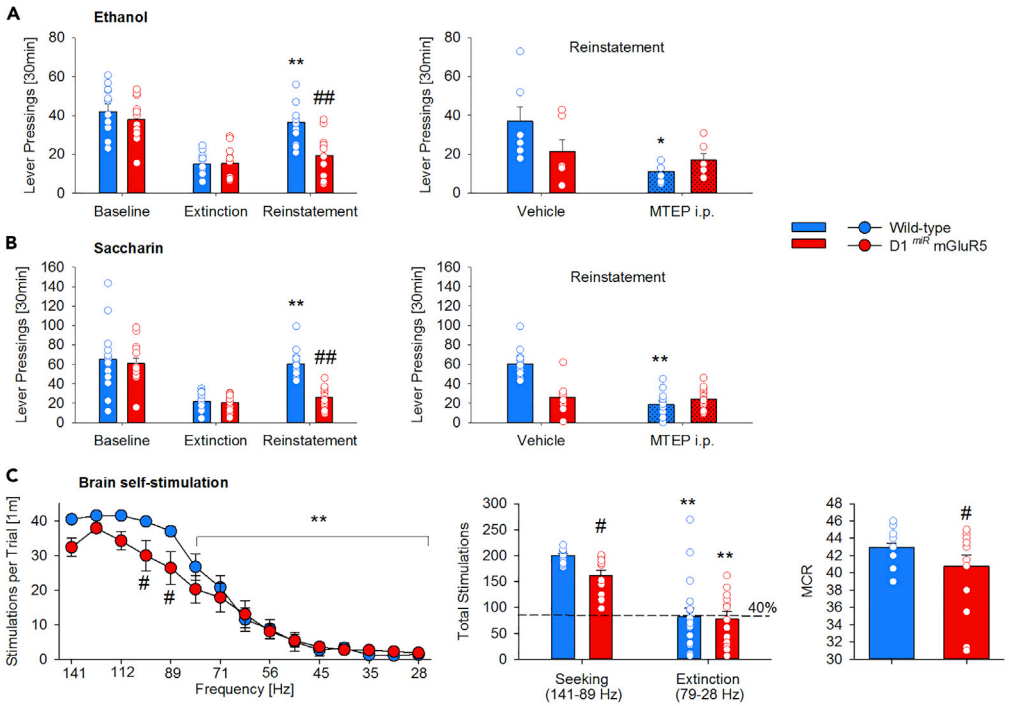

Figure 1. mGluR5 in D1-Containing Neurons Mediates Drug and Natural Reward-Seeking Behavior

Selective genetic deletion of mGluR5 in D1 neurons results in a lack of cue-induced reinstatement of drug- (ethanol (A, left)) and natural (saccharin (B, left); brain stimulation (C)) reward-seeking behavior. Effect of systemic mGluR5 inhibition (MTEP, 20mg/kg, i.p.) on cue-induced reinstatement of ethanol- (A, right) and saccharin (B, right)-seeking behavior in wild-type (n = 6–14) and D1^{miR}mGluR5 (n = 6–14) mice. The lower panel shows the brain stimulation data. During the testing phase of 15 descending frequencies, the first five frequencies were defined as the "seeking" component and the remaining 10 as the "extinction" component (left part). The seeking component of the rate frequency curve (C, middle) and the maximal reinforcement rate (maximum control rate (MCR), C, right) were significantly reduced in the D1^{miR}mGluR5 (n = 13) mice compared with wild-type (n = 18) mice. All data represent mean from 15 mice +SEM. Two-way ANOVA; (*) and (**) corresponds to $p < 0.05$ and 0.0005, respectively vs. extinction, vehicle treatment (A and B) or the first five frequencies (141–89 Hz)/seeking (C); (#), (##) $p < 0.05$ and 0.0005 vs. wild-type mice, respectively.

We further tested a third group of mutant mice for brain stimulation reward using the ICSS paradigm (Bilbao et al., 2015). Following ICSS training animals underwent the testing phase of 15 descending frequencies and all mice showed the expected frequency-dependent decrease in the number of stimulations per trial, which became significant from the sixth frequency on (Figure 1C, left, *frequency* effect $F_{(14,406)} = 119.2$; $p < 0.0001$). Because lower frequencies are less rewarding, and after having observed that from the sixth frequency on the performance of the mice started to decline, we defined the first five frequencies as the "seeking" component of the test and the remaining 10 as the "extinction" component. During the "seeking" component the performance of the D1^{miR}mGluR5 mice was significantly lower than the response rate of the wild-type mice (*genotype* × *frequency* interaction effect $F_{(14,406)} = 2.5$; $p < 0.01$), whereas the "extinction" component was similar in all mice, performing 40% (similar to the extinction in operant conditions) of the baseline (Figure 1C, middle). Furthermore, compared with wild-type, D1^{miR}mGluR5 mice also showed a significantly lower reinforcement rate (Figure 1C, right, $t_{(25)} = 2.1$; $p < 0.05$).

Finally, given the well-known crosstalk between mGluR5 in the MSN and presynaptic CB1R, we also studied the effects of the CB1R antagonist AM251 on cue-induced reinstatement of saccharin-seeking behavior in both wild-type and mutant mice. Similar to MTEP, systemic administration of AM251 reduced the reinstatement in wild-type mice, but not in D1^{miR}mGluR5 mice (Figure S2, *treatment* effect $F_{(1,27)} = 15.3$; $p < 0.001$ and *treatment* × *genotype* interaction effect $F_{(1,27)} = 27.6$; $p < 0.0001$). In order to show that CB1R within the NAc is responsible for the observed effect in wild-type mice, a separate group of wild-type mice received an intra-accumbal administration of AM251. Again this brain-site-specific blockade of CB1R also reduced cue-induced reinstatement of saccharin seeking behavior (Figure S3, $t_{(8)} = 3.7$, $p < 0.01$).

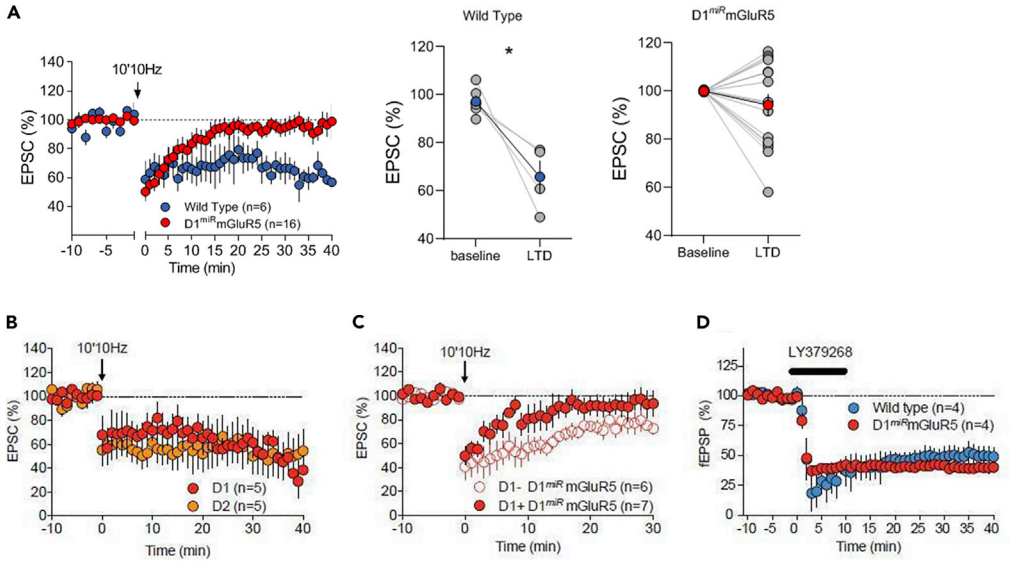

Figure 2. mGluR5 and CB1R in D1 Neurons Mediate eCB-LTD

(A) Genetic downregulation of mGluR5 selectively in D1-MSNs abolishes eCB-mediated long-term depression in the NAc. Average time courses of mean EPSC (represented as percentage of the basal value) showing that in NAc slices prepared from wild-type (WT) and D1^{miR}mGluR5 mice, low-frequency stimulation (10 min 10 Hz, indicated by arrow) induced LTD in WT (n = 6, blue circles) but not in D1^{miR}mGluR5 mice (n = 16, red circles). Error bars indicate SEM, n = individual mouse. Adjacent to the timecourse, individual experiments (blue and red symbols) and group average (black symbols) before (baseline) and after LTD induction are shown. LTD was present in slices from WT mice (on the left) but in contrast, LTD was absent in D1^{miR}mGluR5 mice (on the right). Error bars indicate SEM, n = individual mouse, *p < 0.05, Mann-Whitney U-test.

(B) eCB-LTD is induced in MSNs from both the direct (D1 red) and indirect (D2 orange) pathways in wild-type mice. Retrogradely labeled direct and indirect pathway MSNs (see methods) were visualized by IR-DIC/epifluorescence microscopy and patch clamped.

(C) In D1^{miR}mGluR5 mice, eCB-LTD is selectively abolished in D1+ neurons, as 10-min Hz stimulation (arrow) induces LTD only in D1− (presumably D2+) NAc MSNs (empty red symbols) but is absent in D1+ neurons (filled red circles).

(D) In contrast, bath application of the specific mGluR2/3 agonist, LY379268 (100nM), induces a profound LTD of fEPSP of similar amplitude in NAc of wild-type or D1^{miR}mGluR5 mice. Average time courses of mean EPSC/fEPSP are represented as percentage of basal value.

In summary, mGluR5 in D1-containing neurons mediate in interaction with presynaptic CB1R cocaine- (Novak et al., 2010), ethanol-, saccharin-, and brain-stimulation-seeking responses. However, motor, emotional, and cognitive components can potentially affect reward-seeking responses (Sanchis-Segura and Spanagel, 2006). Therefore, in a series of control experiments, mice were tested for spontaneous locomotor activity, habituation to novelty, anxiety, short-term memory, and other D1-dependent responses. With the exception of a faster habituation to a novel environment (Figure S4B), all tested motor, emotional, or cognitive behaviors were normal in D1^{miR}mGluR5 mice (Figure S4). Next we asked the question which synaptic mechanism could underlie the general lack of reward-seeking responses in D1^{miR}mGluR5 mice.

mGluR5 in D1 Neurons Mediates eCB-LTD

We and others have shown that eCB-LTD requires the postsynaptic activation of mGluR5 to initiate retrograde eCB signaling (Robbe et al., 2002; Katona and Freund, 2012; Zlebnik and Cheer, 2016; Araque et al., 2017). Therefore, we examined basal synaptic transmission and eCB-mediated LTD in D1^{miR}mGluR5 mice in NAc slices. Stimulation mimicking naturally occurring frequencies in NAc MSNs reliably induced a robust eCB-LTD in wild-type but not in D1^{miR}mGluR5 mice (Figure 2A). Given that the deletion of mGluR5 is specific to D1-containing neurons (Novak et al., 2010), we suggest that the lack of eCB-LTD in D1^{miR}mGluR5 mice contributes to the lack of reward seeking in these mice.

Previous reports showed also a prominent eCB-LTD in D2-MSNs in NAc (e.g. Shen et al., 2008; Kreitzer and Malenka, 2007; Grueter et al., 2010; Nazzaro et al., 2012), and this neuronal population may also contribute

to reward-seeking responses (Soares-Cunha et al., 2016). We addressed this issue by specific labeling of MSNs that belong to either the indirect or direct dopamine pathways by using retrobeads. We patched retrogradely labeled direct (thereafter named D1-MSN) and indirect pathway (thereafter named D2-MSN) in wild-type mice and compared the capability of LTD induction in D1-or D2-MSNs in both wild-type and D1^{miR}mGluR5 mice. In line with what has been previously shown eCB-LTD was expressed in direct and indirect pathway MSNs in wild-type animals (Figure 2B). Furthermore, in D1^{miR}mGluR5 mice eCB-LTD was only present in D2-MSNs but not in D1-MSNs (Figure 2C). Taken together, these results suggest that eCB-LTD can be observed in both D1- and D2-MSNs and that we observe a selective lack of eCB-LTD in D1^{miR}mGluR5 mice. If eCB-LTD in D2-MSNs would contribute to a decrease in reward-seeking responses, systemic or accumbal mGluR5 and presynaptic CB1R blockade should have led to an additional decline of responding in D1^{miR}mGluR5 mice. This, however, was not the case (Figures 1, S2, and S3), which led us to the conclusion that eCB-LTD in D2-MSNs play no or an insignificant role in processing of reward-seeking responses, which is also in line with previous studies (Calipari et al., 2016; Hikida et al., 2010; Lobo and Nestler, 2011; Ma et al., 2018; Soares-Cunha et al., 2016).

We have previously shown that both CB1R and mGluR2/3 receptors share the same presynaptic machinery to induce LTD (Mato et al., 2005). To test if mGluR2/3-induced LTD is altered in D1^{miR}mGluR5 mice we examined excitatory postsynaptic currents (EPSCs) in NAc MSNs following bath application of the mGluR2/3 agonist LY379268 and did not observe any genotype difference in LTD induction (Figure 2D), showing that the presynaptic LTD machinery is normal in D1^{miR}mGluR5 mice.

Covariance of presynaptic CB1R functionality and eCB-LTD has been previously reported (Mato et al., 2004; Lafourcade et al., 2011). Thus, we thought to evaluate presynaptic CB1R efficiency in D1^{miR}mGluR5 mice. The dose-response curve for the inhibition of evoked synaptic transmission in response to bath perfusion of the CB1R agonist CP55,940 was shifted to the right in NAc synapses of D1^{miR}mGluR5 mice compared with wild-types (Figure 3J; CP55, 940 0.1 μM; $p < 0.05$) but the maximal inhibition was not significantly reduced (CP55, 940 10 μM; $p = 0.54$). Basal synaptic transmission was also not altered, as administration of a CB1R antagonist did not affect the basal synaptic transmission of both genotypes (Figure S5). These results suggest reduced CB1R expression in D1^{miR}mGluR5 mice. We thus set out to study possible alteration in the eCB machinery on the ultrastructural level in our genetic mouse model.

Deletion of eCB-LTD in the NAc Is a Consequence of Augmented MAGL Activity and Reduced CB1R Expression

CB1R and other components of the eCB system, such as the key enzymes monoacylglycerol lipase (MAGL) (Pan et al., 2011) and diacylglycerol lipase-α (DAGL-α) (Gao et al., 2010), as well as 2-arachidonylglycerol (2-AG) and other eCBs may have been influenced by the constitutive deletion of eCB-LTD in our genetic model. Here we used electron microscopy to analyze the distribution of CB1R, DAGL-α, and MAGL and mass spectrometry to quantify eCBs levels in the NAc of both wild-type and mutant mice.

As described previously (Puente et al., 2011), CB1R labeling was localized at presynaptic terminals making asymmetric synapses with dendritic spines and small dendrites (Figures 3A and 3D). A significant reduction of CB1R immunoparticles in D1^{miR}mGluR5 mice compared with wild-type mice was found on the ultrastructural level within the NAc (Figure 3A, 3D, and 3G, $t_{(13)} = 5.2$, $p < 0.0005$). Hence, reduced presynaptic expression of CB1R correlates with the reduced inhibition of CB1R-dependent excitatory transmission observed in the mutants (Figure 3J). The distribution of DAGL-α and presynaptic MAGL was in agreement with the subcellular pattern in other brain structures (Puente et al., 2011): DAGL-α immunolabeling was mostly distributed in spine head membranes postsynaptic to asymmetric synapses (Figures 3B and 3E), and MAGL immunoparticles were in membranes of excitatory synaptic terminals (Figures 3C and 3F). The proportion of immunoparticles for DAGL-α and presynaptic MAGL did not differ between genotypes (Figure 3G). MAGL was also found at dendritic spines, where it was significantly higher expressed in the mutants (Figure 3G, $t_{(14)} = 2.5$, $p < 0.05$). The significance of a differential distribution of this enzyme (pre- and postsynaptically) and the apparent paradox of increased postsynaptic expression with no changes in DAGL-α is not clear and might indicate non-overlapping functions of this enzyme, which could enable the establishment of two different pools of 2-AG, pre-stored and released, as it has been already suggested (Alger and Kim, 2011). Nevertheless, any possible functional relevance of increased postsynaptic MAGL activity in D1^{miR}mGluR5 to eCB- mediated LTD is unlikely, as the hydrolysis by means of presynaptic MAGL has been proposed as a primary mechanism for 2-AG inactivation (Dinh et al., 2002).

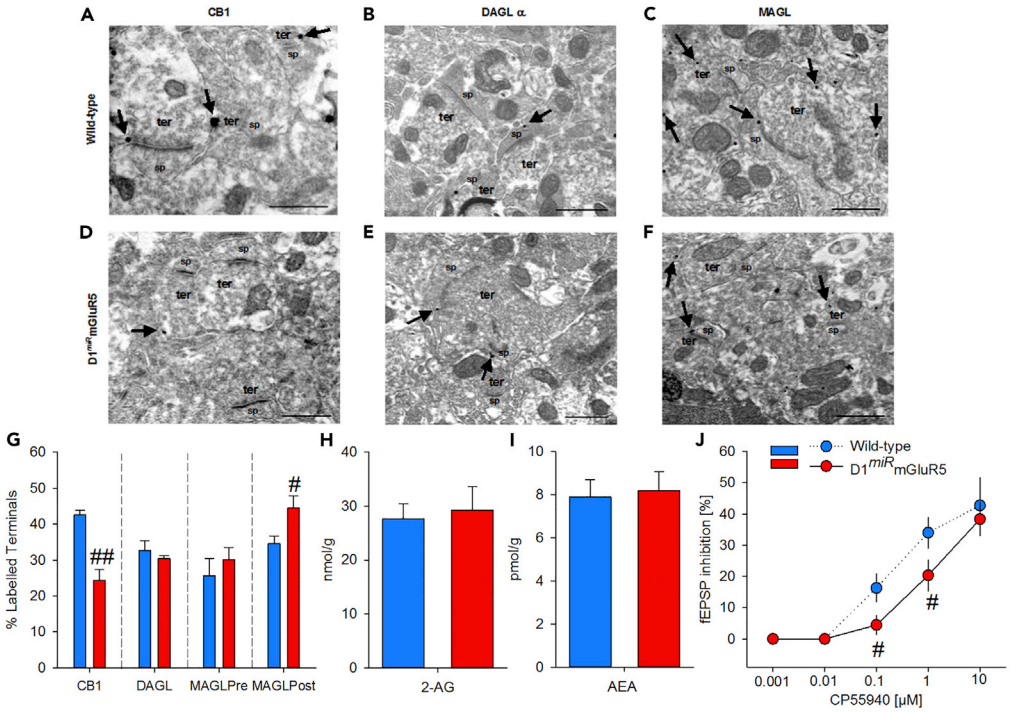

Figure 3. Ultrastructural Changes in the NAc in D1miRmGluR5 Mice

(A–F) Ultrastructural immunolocalization of CB1R, DAGLα, and MAGL in the NAc of wild-type (n = 3, A–C) and D1^{miR}mGluR5 (n = 3, D–F) mice assessed by preembedding silver-intensified immunogold method for electron microscopy. (A and D) CB1R immunoparticles (arrows) are distributed on perisynaptic and extrasynaptic membranes of axon terminals (ter) that make asymmetric synapses with dendritic spines (sp). (B and E) DAGLα immunolabeling is localized in dendritic spine membranes (arrows) away from the postsynaptic densities of asymmetric synapses. (C and F) MAGL shows a presynaptic and postsynaptic localization (arrows) on membranes of asymmetric presynaptic boutons and dendritic spines, respectively.

(G) Proportion of presynaptic and postsynaptic profiles labeled by each antibody for wild-type and D1^{miR}mGluR5 mutant mice. D1^{miR}mGluR5 mice have fewer excitatory synaptic terminals with CB1R but more postsynaptic elements with MAGL receiving asymmetric synapses than wild-type mice.

(H and I) Basal eCB concentrations of 2-arachidonoyl glycerol (2-AG, H) and anandamide (AEA, I) in the NAc are not affected in control (n = 10) and D1^{miR}mGluR5 mice (n = 10).

(J) Bath application of the cannabinoid agonist, CP55, 940, induces a dose-dependent inhibition of evoked fEPSPs recorded in the NAc synapses of wild-type mice, whereas in D1^{miR}mGluR5, there is a shift to the right of the dose-response curve.

Two-way ANOVA, (#) $p < 0.05$, (##) $p < 0.0005$ vs. wild-type. Scale bars 0.5 μm (A–G); picomoles or nanomoles/gram wet tissue +SEM (H and I).

The basal un-stimulated endogenous concentrations of 2-AG and anandamide (AEA) were normal in D1^{miR}mGluR5 mice (Figures 3H and 3I: 2-AG: $t_{(18)} = -0.3$, $p = 0.7$; AEA: $t_{(18)} = -0.2$, $p = 0.8$). Neither 2-AG and AEA nor the metabolites 1-arachidonoyl glycerol (1-AG), arachidonic acid (AA), and other eCB congener concentrations, including oleoylethanolamide (OEA) and palmitoylethanolamide (PEA), (Figure S6) were affected. This finding is in line with the overall normal expression levels of the key enzymes in the mutant mice and supports the assertion that 2-AG levels are solely determined by the balance between production (DAGL- α) and presynaptic degradation by MAGL (Ohno-Shosaku et al., 2012). In summary, these ultrastructural data show that an augmented postsynaptic MAGL activity, combined with reduced CB1R and a lack of mGluR5, is the molecular alterations that result in a lack of eCB-LTD. One possibility to counteract these molecular alterations and to restore eCB-LTD is by increasing 2-AG levels (Bosch-Bouju et al., 2016).

Enhancement of eCB Signaling Restores eCB-LTD and Reward-Seeking Responses in D1^{miR}mGluR5

The MAGL inhibitor JZL184 produces a selective blockade of 2-AG hydrolysis and thereby leads to an increase in 2-AG levels (Long et al., 2009; Bosch-Bouju et al., 2016). JZL184 (1 mM) restored eCB-LTD in the

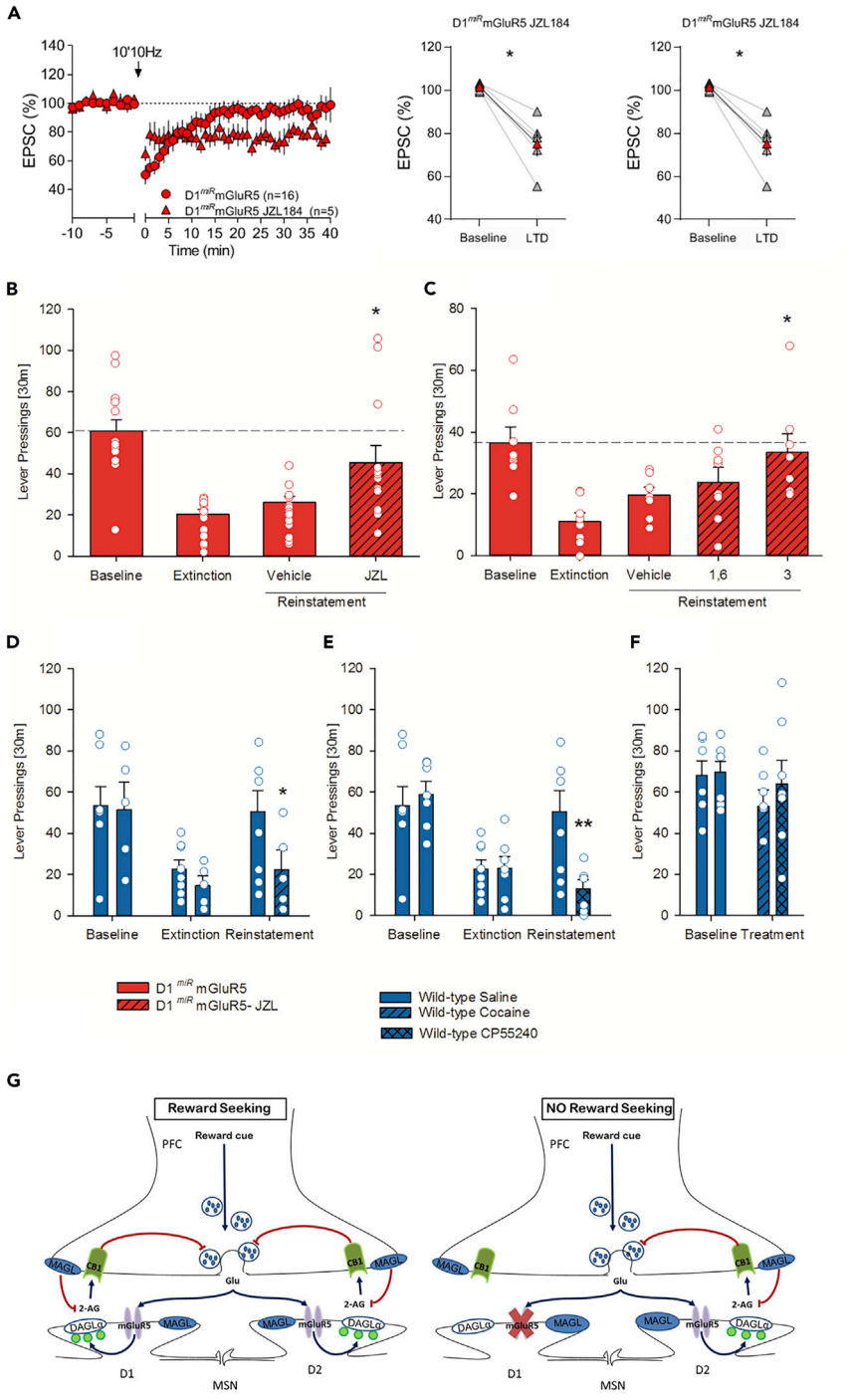

Figure 4. Rescue of Genetically Abolished eCB-LTD and Reward-seeking Behavior

(A) Average time-courses of mean EPSC (represented as percentage of the basal value) showing that in NAc slices prepared from D1^{miR}mGluR5 mice, low-frequency stimulation (10min 10 Hz, indicated by arrow) induced LTD in the presence of the MAGL inhibitor, JZL184 (1μM, red triangles, n = 5 mice) but not in untreated slices (red circles, n = 16 mice). Adjacent to the timecourse, individual experiments (red symbols) and group average (black symbols) before (baseline) and after LTD induction are shown. LTD is absent in untreated slices (on the left). In contrast, LTD was present in slices pretreated with JZL184 (on the right). Error bars indicate SEM, n = individual mouse, *p < 0.05, Mann-Whitney U-test.

Figure 4. *Continued*

(B) Effects of MAGL inhibition on cue-induced reinstatement of saccharin-seeking behavior. Increasing 2-AG levels by administration of the MAGL inhibitor JZL 184 (16 mg/kg, i.p.; n = 15), produces a complete rescue of the reinstatement response in the D1*miR*mGluR5 mice.

(C–F) (C) Intra-accumbal administration of JZL 184 into the NAc core of D1^{miR}mGluR5 mice resulted in a dose-dependent rescue of the reinstatement response. Behaviorally, pharmacological blockade of eCB-LTD by cocaine (n = 6–7) or the CB1 agonist CP55,940 (n = 7) selectively abolished saccharin-seeking behavior triggered by the conditioned cues in wild-type mice (D, E), whereas it did not affect saccharin self-administration (F).

(G) Accumbal D1 eCB-LTD is the physiological substrate for reward-seeking behavior. Graphic summary (G) showing the mechanism of reward seeking driven by accumbal D1-eCB-LTD. (Left) Presentation of the conditioned cue stimulates prefrontal cortico-accumbal glutamatergic neurons, glutamate is released into the synaptic space, and stimulation of mGluR5 of D1-containing MSNs triggers the synthesis and release of 2-AG through the DAGL pathway (blue arrows). Released 2-AG retrogradely activates CB1Rs in the presynaptic neuron (blue arrow), which in turn results in LTD, and thus a persistent reduction of synaptic neurotransmission (glutamate release, red arrow). This reduction on synaptic transmission might induce a "craving" state and participate to the seeking response. (Right) In D1^{miR}mGluR5, presentation of the cue activates mGluR5-dependent perisynaptic signaling machinery (the synthesis and release of 2-AG through the diacylglycerol pathway) only in D2 neurons, not in D1 neurons. Without this D1-dependent LTD, seeking behavior is not triggered. Blue arrows indicate activation, and red arrows indicate inhibition.

All data represent mean ± SEM. Two-way ANOVA, (*) $p < 0.05$ and (**) $p < 0.01$ vs. vehicle treatment, respectively.

NAc in D1^{miR}mGluR5 (Figure 4A). Likewise, systemic application of JZL184 prior to the reinstatement led to a saccharin-seeking response in D1^{miR}mGluR5 mice (Figure 4B, $t_{(2.8)} = -2.8$, $p < 0.05$), which was comparable to the one observed in wild-type mice. In wild-type mice the reinstatement response was attenuated by JZL184 (Figure S7, $t_{(13)} = 9.2$, $p < 0.0001$), possibly due to the functional desensitization of CB1R in response to elevated 2-AG levels (Long et al., 2009) or due to the rewarding properties of enhanced endogenous 2-AG levels (Justinova et al., 2005), and subsequent CB1R stimulation. As a proof of concept experiments, we sought to demonstrate a direct role of the NAc by infusing JZL184 into this brain site. JZL184 dose-dependently restored the reinstatement response (Figure 4C, $t_{(7)} = 3.4$, $p < 0.05$ and $t_{(7)} = 4.4$, $p < 0.01$ for 1.6 and 3μg/0.5μL, respectively). Taken together, these data show that increasing 2-AG levels and thereby CB1R signaling in the NAc restores e-CB-LTD in D1^{miR}mGluR5 mice and subsequently reward-seeking responses.

If eCB-LTD in D1-containing neurons is the physiological substrate of reward-seeking behavior, one should be able to manipulate reward-seeking by prior drug administration. Thus, it has been shown that already a single *in vivo* exposure to cocaine (Fourgeaud et al., 2004) or Δ9-THC (Mato et al., 2004) abolishes eCB-LTD in the NAc. Therefore, acute drug treatment that ablates eCB-LTD should impede reward seeking in wild-type mice. Indeed, a single cocaine or CP55,940 injection 24 h before reinstatement testing—a protocol that abolishes eCB-LTD—selectively inhibited cue-induced saccharin-seeking responses (Figure 4D, ANOVA, for cocaine: *reinstatement* effect: $F_{(2,22)} = 11.9$, $p < 0.001$; *reinstatement* × *treatment* interaction effect: $F_{(4,34)} = 4.5$, $p < 0.01$; Figure 4E, for CP55,940: *reinstatement* effect: $F_{(2,26)} = 16.9$, $p < 0.0001$; *reinstatement* × *treatment* interaction effect: $F_{(2,26)} = 7.7$, $p < 0.005$) but not self-administration (Figure 4F, *self-administration* effect: $F_{(1,11)} = 3.7$, $p = 0.08$; *treatment* effect: $F_{(1,11)} = 0.3$, $p = 0.6$) in wild-type mice. This is a finding with clinical implications, as it would suggest that acute forced drug administration abolishes craving for an alternative reinforcer on subsequent days. This observation deserves closer investigations, especially in relevance for human drug-taking behavior.

DISCUSSION

Here we propose a model (Figure 4G) in which the presentation of drug-conditioned cues activate excitatory afferents to the NAc and facilitate drug and natural reward-seeking responses by encoding reward-associated cues (Britt et al., 2012). This excitation leads to an increase of accumbal glutamate transmission (Kalivas, 2009) and activation of postsynaptic mGluR5 on D1-MSNs. Subsequent mGluR5-mediated eCB-LTD within the NAc leads then to an inhibition of cue-induced glutamate release and finally to a state of seeking for the reward-associated cue. The selective inhibition of glutamate transmission might not take place when key players such as CB1R and mGluR5 are pharmacologically blocked or genetically manipulated as in our D1^{miR}mGluR5 mutants. Hence in D1^{miR}mGluR5 mice, presentation of a reward-associated cue does not activate the mGluR5-dependent perisynaptic signaling machinery; i.e., the synthesis and release of 2-AG through the diacylglycerol pathway (Hashimotodani et al., 2007). A downregulation of CB1R from glutamatergic terminals ultimately results in an impairment of long-term control of glutamate

release by a lack of D1-MSN mediated LTD induction. Without this LTD, seeking behavior in these mutant mice is not triggered.

Our data are compatible with the idea that both D1- and D2 (as well as D1/D2)-expressing neurons produce 2-AG in the NAc. We propose that in wild-type mice, D1 and D1/D2 MSNs are a principal source of the 2-AG that mediates eCB-LTD and reward-seeking responses. In our D1^{miR}mGluR5 mutants, the production of 2-AG is insufficient to reach the threshold of LTD induction. In the presence of JZL184, 2-AG is augmented and sufficient to trigger LTD. This idea in line with a recent study shows that mGluR5 antagonism inhibits cocaine reinforcement and relapse by elevation of extracellular glutamate in the NAc via a CB1 receptor mechanism (Li et al., 2018).

The possibility that D2-MSN in the NAc core could have also contributed to the alterations in reward-seeking responses in mutant mice is unlikely because a previous study by Anderson et al. (2006) showed that cooperative activation of D1-like and D2-like dopamine receptors is required for the reinstatement of a drug-seeking behavior in the NAc shell, but not core. Furthermore, neither systemic nor accumbal mGluR5 or presynaptic CB1R blockade led to a further decrease in D1^{miR}mGluR5 mutants (Figure 1, S2, and S3). This suggests that eCB-LTD in D2-MSNs plays no or only a minor role in the processing of reward-seeking responses, which is also in line with previous studies (Calipari et al., 2016; Hikida et al., 2010; Lobo and Nestler, 2011; Ma et al., 2018; Soares-Cunha et al., 2016).

In conclusion, we show that mGluR5 interacts with the eCB system to induce synaptic changes in D1 neurons in the NAc and that the resulting eCB-LTD mediates cue-induced reward-seeking responses. We propose that such molecular and synaptic events contribute to the common neural circuit adaptations that underlie the persistence of natural and drug reward memories. Cues paired with drugs of abuse can drive behavioral and physiological responses responsible for craving and relapse even after long periods of abstinence (Shaham et al., 2003; Sanchis-Segura and Spanagel, 2006), and similarly, cues conditioned to non-drug rewards such as highly palatable liquids and food, sex, and money induce similar network activity and contribute to overeating, obesity, gambling, and other forms of addictive behavior (Noori et al., 2016). Proposing that natural and drug rewards share the same molecular and physiological correlate for cue-induced reward-seeking responses, medications targeting mGluR5-dependent eCB-LTD, such as compounds that modulate endogenous 2-AG levels, may be useful in treating a variety of addictive behaviors.

Limitations of the Study

The present study has two limitations. First, with our mouse model we could not well distinguish about the contribution of D1- and D2-MSNs in the processing of reward-seeking responses. Although our data strongly support the conclusion that eCB-LTD in D2-MSNs plays no important role in processing of reward-seeking responses, the use of D2miRmGluR5 mutants would have provided full evidence for this conclusion. Clearly, the generation of such a selective transgenic mouse model and its full behavioral, molecular, neuroanatomical, and physiological characterization as presented here for D1miRmGluR5 mutants would have been a major contribution on its own. Secondly, we did not perform slice experiments to test if saccharin exposure can abolish eCB-LTD. This research question was indeed of interest in regard to our previous publications where we showed that eCB-mediated synaptic plasticity in the NAc is eliminated following exposure to drugs of abuse (Mato et al., 2004; Fourgeaud et al., 2004; Zlebnik and Cheer, 2016). However, in the context of this study, this additional information would not have impact on our conclusions: the present work tested the hypothesis that eCB-LTD in D1 MSN mediates reward-seeking behavior and not that natural rewards would abolish this form of plasticity.

METHODS

All methods can be found in the accompanying Transparent Methods supplemental file.

SUPPLEMENTAL INFORMATION

Supplemental Information can be found online at https://doi.org/10.1016/j.isci.2020.100951.

ACKNOWLEDGMENTS

We would like to thank Rick Bernardi for editing this manuscript and Anne Rohrbacher for tissue preparation. This work was supported by the BundesministeriumfürBildung und Forschung (e:Med program;

FKZ: 01ZX1311A and 01ZX1909, Spanagel et al., 2013) and the Deutsche Forschungsgemeinschaft (DFG, Germany) TRR265/A05 and SFB1158/B04. Work in O.J.M. laboratory is supported by INSERM. C.S. and R.L were supported by the DFG Research Unit FOR926 (central project CP1) and by the BMBF Consortium LOGIN. Funding for P.G.'s laboratory was provided by Red de TrastornosAdictivos, ISCIII ("RD16/0017/0012" to PG), co-funded by ERDF/ESF, "Investing in your future"; The Basque Government (IT1230-19) and MINECO/FEDER, UE (SAF2015-65034-R).

AUTHOR CONTRIBUTIONS

A.B., M.E., S.P.W., S.L., and R.S. performed and analyzed the behavioral experiments. A.T., D.N., O.L., M.S and O.M performed and analyzed the electrophysiology experiments. A.T. prepared the original electrophysiology figures, drafted an early version of the manuscript and participated to the manuscript's correction. A.R.V., N.P., and P.G. performed and analyzed the immunohistochemistry for electron microscopy experiment. R.L. and B.L. performed and analyzed the measurement of eCB levels. A.B., O.M., and R.S. are accountable for the integrity of the data reported in the paper, carried out the analysis, and wrote the manuscript; all of the authors participated in the design and analysis of experiments and in editing of the paper.

DECLARATION OF INTERESTS

The authors declare no competing interests.

Received: July 12, 2017
Revised: August 15, 2019
Accepted: February 24, 2020
Published: March 27, 2020

REFERENCES

Adams, C.L., Short, J.L., and Lawrence, A.J. (2010). Cue-conditioned alcohol seeking in rats following abstinence: involvement of metabotropic glutamate 5 receptors. Br. J. Pharmacol. *159*, 534–542.

Alger, B.E., and Kim, J. (2011). Supply and demand for endocannabinoids. Trends Neurosci. *34*, 304–315.

Alvarez-Jaimes, L., Polis, I., and Parsons, L.H. (2008). Attenuation of cue-induced heroin-seeking behavior by cannabinoid CB1 antagonist infusions into the nucleus accumbens core and prefrontal cortex, but not basolateral amygdala. Neuropsychopharmacology *10*, 2483–2489.

Anderson, S.M., Schmidt, H.D., and Pierce, R.C. (2006). Administration of the D2 dopamine receptor antagonist sulpiride into the shell, but not the core, of the nucleus accumbens attenuates cocaine priming-induced reinstatement of drug seeking. Neuropsychopharmacology *31*, 1452–1461.

Araque, A., Castillo, P.E., Manzoni, O.J., and Tonini, R. (2017). Synaptic functions of endocannabinoid signaling in health and disease. Neuropharmacology *124*, 13–24.

Bäckström, P., Bachteler, D., Koch, S., Hyytiä, P., and Spanagel, R. (2004). mGluR5 antagonist MPEP reduces ethanol-seeking and relapse behavior. Neuropsychopharmacology *29*, 921–928.

Bilbao, A., Robinson, J.E., Heilig, M., Malanga, C.J., Spanagel, R., Sommer, W.H., and Thorsell, A. (2015). A pharmacogenetic determinant of mu-opioid receptor antagonist effects on alcohol reward and consumption: evidence from humanized mice. Biol. Psychiatry *77*, 850–858.

Bosch-Bouju, C., Larrieu, T., Linders, L., Manzoni, O.J., and Layé, S. (2016). Endocannabinoid-mediated plasticity in nucleus accumbenscontrols vulnerability to anxiety after social defeat stress. Cell Rep. *16*, 1237–1242.

Britt, J.P., Benaliouad, F., McDevitt, R.A., Stuber, G.D., Wise, R.A., and Bonci, A. (2012). Synaptic and behavioral profile of multiple glutamatergic inputs to the nucleus accumbens. Neuron *76*, 790–803.

Calipari, E.S., Bagot, R.C., Purushothaman, I., Davidson, T.J., Yorgason, J.T., Peña, C.J., Walker, D.M., Pirpinias, S.T., Guise, K.G., Ramakrishnan, C., et al. (2016). In vivo imaging identifies temporal signature of D1 and D2 medium spiny neurons in cocaine reward. Proc. Natl. Acad. Sci. U S A *113*, 2726–2731.

Cippitelli, A., Bilbao, A., Hansson, A.C., del Arco, I., Sommer, W.H., Heilig, M., Massi, M., Bermúdez-Silva, F.J., Navarro, M., Ciccocioppo, R., et al. (2005). Cannabinoid CB1 receptor antagonism reduces conditioned reinstatement of ethanol-seeking behavior in rats. Eur. J. Neurosci. *21*, 2243–2251.

Cleva, R.M., Watterson, L.R., Johnson, M.A., and Olive, M.F. (2012). Differential modulation of thresholds for intracranial self-stimulation by mGlu5 positive and negative allosteric modulators: implications for effects on drug self-administration. Front. Pharmacol. *2*, 93.

Dinh, T.P., Freund, T.F., and Piomelli, D. (2002). A role for monoglyceride lipase in 2-arachidonoylglycerol inactivation. Chem. Phys. Lipids *121*, 149–158.

Eisenhardt, M., Leixner, S., Luján, R., Spanagel, R., and Bilbao, A. (2015). Glutamate receptors within the mesolimbic dopamine system mediate alcohol relapse behavior. J. Neurosci. *35*, 15523–15538.

Fattore, L., Fadda, P., and Fratta, W. (2007). Endocannabinoid regulation of relapse mechanisms. Pharmacol. Res. *56*, 418–427.

Fourgeaud, L., Mato, S., Bouchet, D., Hémar, A., Worley, P.F., and Manzoni, O.J. (2004). A single in vivo exposure to cocaine abolishes endocannabinoid-mediated long-term depression in the nucleus accumbens. J. Neurosci. *24*, 6939–6945.

Gao, Y., Vasilyev, D.V., Goncalves, M.B., Howell, F.V., Hobbs, C., Reisenberg, M., Shen, R., Zhang, M.Y., Strassle, B.W., Lu, P., et al. (2010). Loss of retrograde endocannabinoidsignaling and reduced adult neurogenesis in diacylglycerol lipase knock-out mice. J. Neurosci. *30*, 2017–2024.

Grueter, B.A., Brasnjo, G., and Malenka, R.C. (2010). Postsynaptic TRPV1 triggers cell type-specific long-term depression in the nucleus accumbens. Nat. Neurosci. *13*, 1519–1525.

Hashimotodani, Y., Ohno-Shosaku, T., and Kano, M. (2007). Ca2+-assisted receptor-driven endocannabinoid release: mechanisms that associate presynaptic and postsynaptic activities. Curr. Opin. Neurobiol. *17*, 360–365.

Hikida, T., Kimura, K., Wada, N., Funabiki, K., and Nakanishi, S. (2010). Distinct roles of synaptic

transmission in direct and indirect striatal pathways to reward and aversive behavior. Neuron *66*, 896–907.

Justinova, Z., Solinas, M., Tanda, G., Redhi, G.H., and Goldberg, S.R. (2005). The endogenous cannabinoid anandamide and its synthetic analog R(+)-methanandamide are intravenously self-administered by squirrel monkeys. J. Neurosci. *25*, 5645–5650.

Kalivas, P.W. (2009). The glutamate homeostasis hypothesis of addiction. Nat. Rev. Neurosci. *10*, 561–572.

Katona, I., and Freund, T.F. (2012). Multiple functions of endocannabinoid signaling in the brain. Annu. Rev. Neurosci. *35*, 529–558.

Knackstedt, L.A., Trantham-Davidson, H.L., and Schwendt, M. (2014). The role of ventral and dorsal striatum mGluR5 in relapse to cocaine-seeking and extinction learning. Addict. Biol. *19*, 87–101.

Kodas, E., Cohen, C., Louis, C., and Griebel, G. (2007). Cortico-limbic circuitry for conditioned nicotine-seeking behaviour in rats involves endocannabinoidsignalling. Psychopharmacology (Berl) *194*, 161–171.

Kreitzer, A.C., and Malenka, R.C. (2007). Endocannabinoid-mediated rescue of striatal LTD and motor deficits in Parkinson's disease models. Nature *445*, 643–647.

Lafourcade, M., Larrieu, T., Mato, S., Duffaud, A., Sepers, M., Matias, I., De Smedt-Peyrusse, V., Labrousse, V.F., Bretillon, L., Matute, C., et al. (2011). Nutritional omega-3 deficiency abolishes endocannabinoid-mediated neuronal functions. Nat. Neurosci. *14*, 345–350.

Li, X., Peng, X.Q., Jordan, C.J., Li, J., Bi, G.H., He, Y., Yang, H.J., Zhang, H.Y., Gardner, E.L., and Xi, Z.X. (2018). mGluR5 antagonism inhibits cocaine reinforcement and relapse by elevation of extracellular glutamate in the nucleus accumbens via a CB1 receptor mechanism. Sci. Rep. *8*, 3686.

Lobo, M.K., and Nestler, E.J. (2011). The striatal balancing act in drug addiction: distinct roles of direct and indirect pathway medium spiny neurons. Front. Neuroanat. *5*, 41.

Long, J.Z., Li, W., Booker, L., Burston, J.J., Kinsey, S.G., Schlosburg, J.E., Pavón, F.J., Serrano, A.M., Selley, D.E., Parsons, L.H., et al. (2009). Selective blockade of 2-arachidonoylglycerol hydrolysis produces cannabinoid behavioral effects. Nat. Chem. Biol. *5*, 37–44.

Lüscher, C., and Malenka, R.C. (2011). Drug-evoked synaptic plasticity in addiction: from molecular changes to circuit remodelling. Neuron *69*, 650–663.

Ma, T., Cheng, Y., Roltsch, E., Wang, X., Lu, J., Gao, X., Huang, C.C.Y., Wei, X.Y., Ji, J.Y., and Wang, J. (2018). Bidirectional and long-lasting control of alcohol-seeking behavior by corticostriatal LTP and LTD. Nat.Neurosci. *21*, 373–383.

Mato, S., Chevaleyre, V., Robbe, D., Pazos, A., Castillo, P.E., and Manzoni, O.J. (2004). A single in-vivo exposure to delta 9THC blocks endocannabinoid-mediated synaptic plasticity. Nat. Neurosci. *6*, 585–586.

Mato, S., Robbe, D., Grandes, P., and Manzoni, O.J. (2005). Presynaptic homeostatic plasticity rescues long-term depression after chronic Delta 9-tetrahydrocannabinol exposure. J. Neurosci *25*, 11619–11627.

Mihov, Y., and Hasler, G. (2016). Negative allosteric modulators of metabotropic glutamate receptors subtype 5 in addiction: a therapeutic window. Int. J. Neuropsychopharmacol. *19*, pii: pyw002.

Nazzaro, C., Greco, B., Cerovic, M., Baxter, P., Rubino, T., Trusel, M., Parolaro, D., Tkatch, T., Benfenati, F., Pedarzani, P., et al. (2012). SK channel modulation rescues striatal plasticity and control over habit in cannabinoid tolerance. Nat. Neurosci. *15*, 284–293.

Noori, H.R., CosaLinan, A., and Spanagel, R. (2016). Largely overlapping neuronal substrates of reactivity to drug, gambling, food and sexual cues: a comprehensive meta-analysis. Eur. Neuropsychopharmacol. *26*, 1419–1430.

Novak, M., Halbout, B., O'Connor, E.C., Rodriguez Parkitna, J., Su, T., Chai, M., Crombag, H.S., Bilbao, A., Spanagel, R., Stephens, D.N., et al. (2010). Incentive learning underlying cocaine-seeking requires mGluR5 receptors located on dopamine D1 receptor-expressing neurons. J. Neurosci. *30*, 11973–11982.

Ohno-Shosaku, T., Tanimura, A., Hashimotodani, Y., and Kano, M. (2012). Endocannabinoids and retrograde modulation of synaptic transmission. Neuroscientist *18*, 119–132.

Olive, M.F. (2009). Metabotropic glutamate receptor ligands as potential therapeutics for addiction. Curr. Drug Abuse Rev. *2*, 83–98.

Pan, B., Wang, W., Zhong, P., Blankman, J.L., Cravatt, B.F., and Liu, Q.S. (2011). Alterations of endocannabinoid signaling, synaptic plasticity, learning, and memory in monoacylglycerol lipase knock-out mice. J. Neurosci. *31*, 13420–13430.

Puente, N., Cui, Y., Lassalle, O., Lafourcade, M., Georges, F., Venance, L., Grandes, P., and Manzoni, O.J. (2011). Polymodal activation of the endocannabinoid system in the extended amygdala. Nat. Neurosci. *12*, 1542–1547.

Robbe, D., Kopf, M., Remaury, A., Bockaert, J., and Manzoni, O.J. (2002). Endogenous cannabinoids mediate long-term synaptic depression in the nucleus accumbens. Proc. Natl. Acad. Sci. U S A *99*, 8384–8388.

Russo, S.J., Dietz, D.M., Dumitriu, D., Morrison, J.H., Malenka, R.C., and Nestler, E.J. (2010). The addicted synapse: mechanisms of synaptic and structural plasticity in nucleus accumbens. Trends Neurosci. *33*, 267–276.

Sanchis-Segura, C., and Spanagel, R. (2006). Behavioural assessment of drug reinforcement and addictive features in rodents: an overview. Addict. Biol. *11*, 2–38.

Sanchis-Segura, C., Cline, B.H., Marsicano, G., Lutz, B., and Spanagel, R. (2004). Reduced sensitivity to reward in CB1 knockout mice. Psychopharmacology (Berl) *176*, 223–232.

Schmidt, H.D., Kimmey, B.A., Arreola, A.C., and Pierce, R.C. (2015). Group I metabotropic glutamate receptor-mediated activation of PKC gamma in the nucleus accumbens core promotes the reinstatement of cocaine seeking. Addict. Biol. *20*, 285–296.

Shaham, Y., Shalev, U., Lu, L., De Wit, H., and Stewart, J. (2003). The reinstatement model of drug relapse: history, methodology and major findings. Psychopharmacology (Berl) *168*, 3–20.

Shen, W., Flajolet, M., Greengard, P., and Surmeier, D.J. (2008). Dichotomous dopaminergic control of striatal synaptic plasticity. Science *321*, 848–851.

Sinclair, C.M., Cleva, R.M., Hood, L.E., Olive, M.F., and Gass, J.T. (2012). mGluR5 receptors in the basolateral amygdala and nucleus accumbens regulate cue-induced reinstatement of ethanol-seeking behavior. Pharmacol. Biochem. Behav. *101*, 329–335.

Soares-Cunha, C., Coimbra, B., Sousa, N., and Rodrigues, A.J. (2016). Reappraising striatal D1- and D2-neurons in reward and aversion. Neurosci. Biobehav. Rev. *68*, 370–386.

Spanagel, R., Durstewitz, D., Hansson, A., Heinz, A., Kiefer, F., Köhr, G., Matthäus, F., Nöthen, M.M., Noori, H.R., Obermayer, K., et al. (2013). A systems medicine research approach for studying alcohol addiction. Addict. Biol. *18*, 883–896.

De Vries, T.J., Shaham, Y., Homberg, J.R., Crombag, H., Schuurman, K., Dieben, J., Vanderschuren, L.J., and Schoffelmeer, A.N. (2001). A cannabinoid mechanism in relapse to cocaine seeking. Nat. Med. *7*, 1151–1154.

Wang, X., Moussawi, K., Knackstedt, L., Shen, H., and Kalivas, P.W. (2013). Role of mGluR5 neurotransmission in reinstated cocaine-seeking. Addict. Biol. *18*, 40–49.

Watterson, L.R., Kufahl, P.R., Nemirovsky, N.E., Sewalia, K., Hood, L.E., and Olive, M.F. (2013). Attenuation of reinstatement of methamphetamine-, sucrose-, and food-seeking behavior in rats by fenobam, a metabotropic glutamate receptor 5 negative allosteric modulator. Psychopharmacology *225*, 151–159.

Xi, Z.X., Gilbert, J.G., Peng, X.Q., Pak, A.C., Li, X., and Gardner, E.L. (2006). Cannabinoid CB1 receptor antagonist AM251 inhibits cocaine-primed relapse in rats: role of glutamate in the nucleus accumbens. J. Neurosci. *26*, 8531–8536.

Zlebnik, N.E., and Cheer, J.F. (2016). Drug-induced alterations of endocannabinoid-mediated plasticity in brain reward regions. J. Neurosci. *36*, 10230–10238.

iScience, Volume *23*

Supplemental Information

Endocannabinoid LTD in Accumbal D1 Neurons

Mediates Reward-Seeking Behavior

Ainhoa Bilbao, Daniela Neuhofer, Marja Sepers, Shou-peng Wei, Manuela Eisenhardt, Sarah Hertle, Olivier Lassalle, Almudena Ramos-Uriarte, Nagore Puente, Raissa Lerner, Pedro Grandes, Beat Lutz, Olivier J. Manzoni, and Rainer Spanagel

Supplemental Figure 1

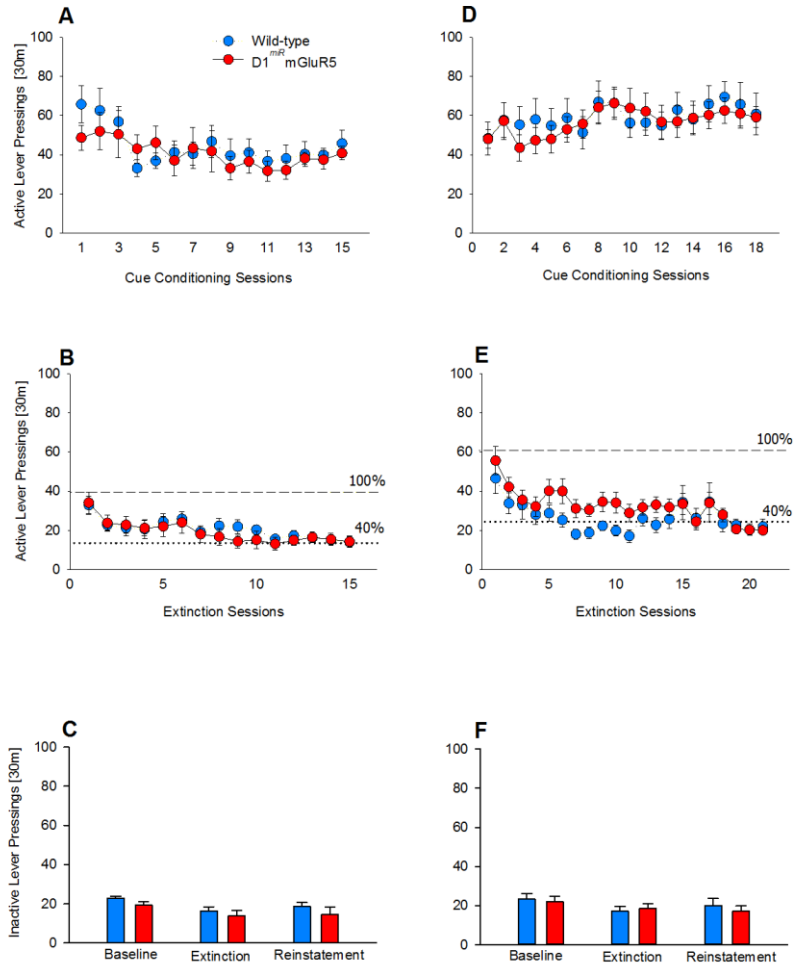

Figure S1. Active and inactive lever pressing for operant self-administration during training and extinction phases, related to Figure 1.

(A) Operant lever press responses across 15 daily sessions of contextual cues (S^+/CS^+) pairings with a 10% ethanol solution are stable and do not significantly differ between wild-type and $D1^{miR}$mGluR5 mice (n=12 per genotype). (B) Extinction is achieved after 15 sessions and does not differ between the two genotypes. (C) Inactive lever pressing during the S^+/CS^+ conditions (during the last 3 days of the training phase), the extinction phase and during the reinstatement test are similar in both genotypes (D) Operant lever responses for the natural reward saccharin did not differ in wild-type (n=14) and $D1^{miR}$mGluR5 mice (n=15). (E) Extinction is achieved after 21 sessions and does not differ between the two genotypes. (F) Inactive lever pressing during the S^+/CS^+ conditions (during the last 3 days of the training phase), the extinction phase and during the reinstatement test are similar in both genotypes. Data represent mean ± SEM.

Supplemental Figure 2

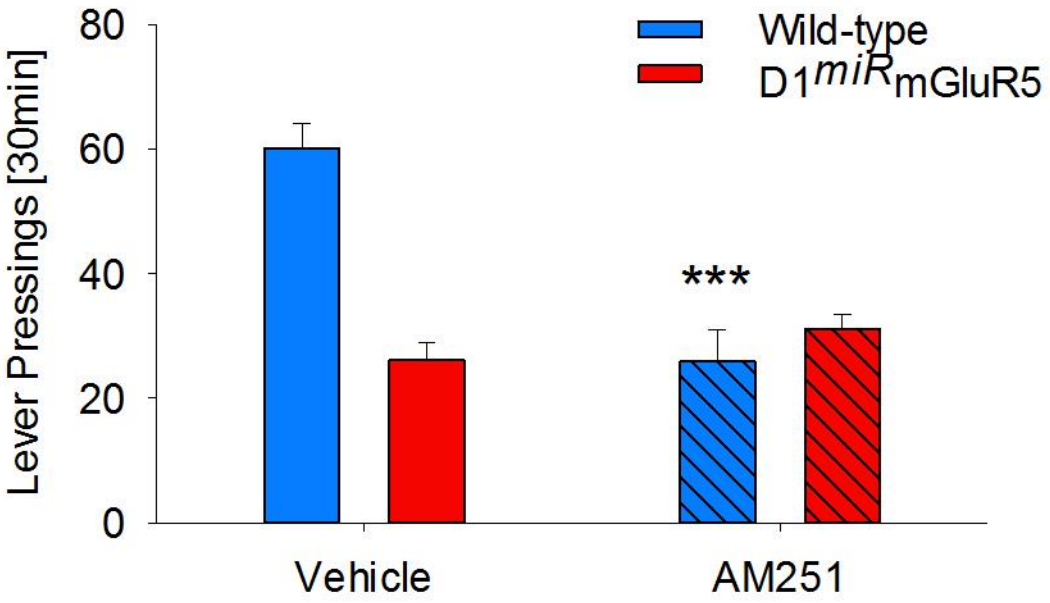

Figure S2. Effect of systemic administration of the CB1 antagonist AM251 on cue-induced reinstatement of saccharin-seeking behavior, related to Figure 1.

Systemic administration of AM251 reduced the reinstatement in wild-type mice, but not in D1^{miR}mGluR5 mice. Data represent mean ± SEM. Two-way ANOVA, (*) P <0.001 vs vehicle treatment.

Supplemental Figure 3

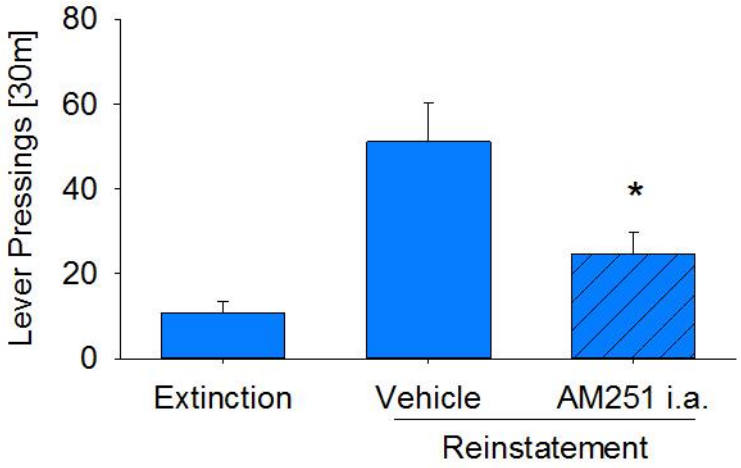

Figure S3. Effect of accumbal inhibition of CB1 on cue-induced reinstatement of saccharin seeking, related to Figure 1. Effect of accumbal inhibition of CB1 (1µg/0.5µl AM251, intra-accumbal) on cue-induced reinstatement of saccharin seeking in wild-type (n=9) mice. Data represent mean ± SEM. Two-way ANOVA, (*) P <0.001 vs vehicle treatment.

Supplemental Figure 4

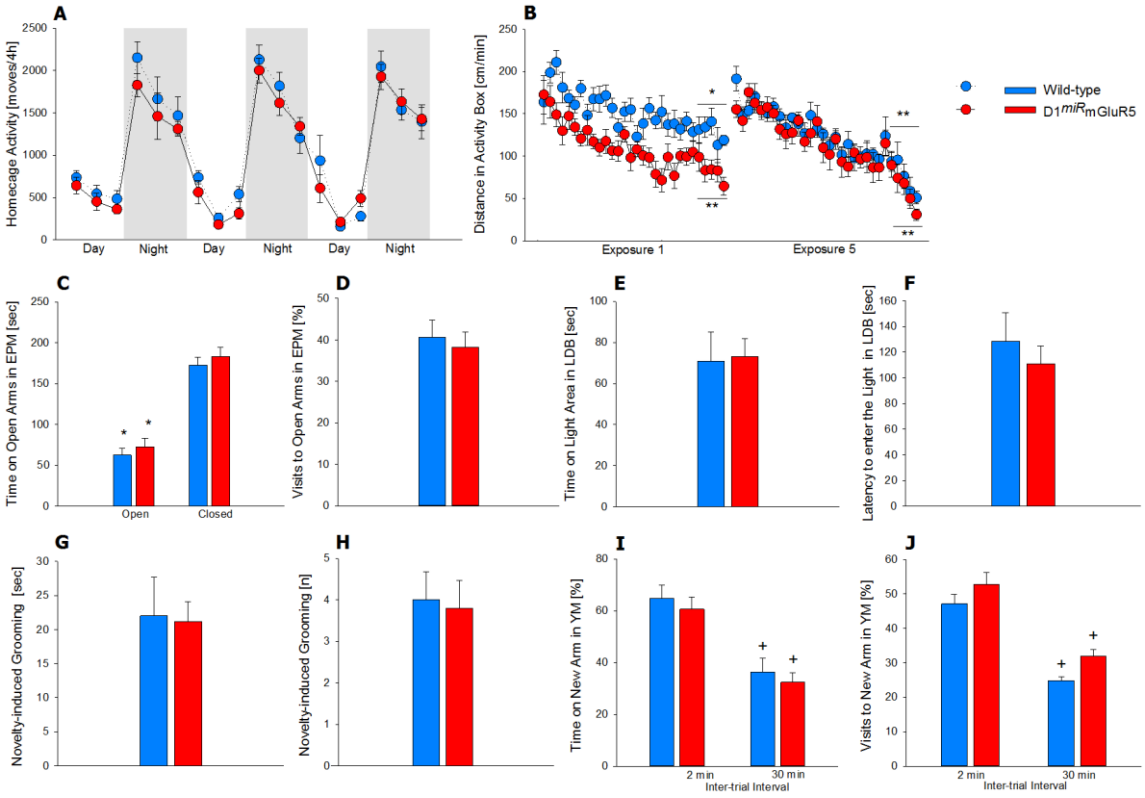

Figure S4. Locomotor activity, anxiety and short-term memory are intact in D1^{miR}mGluR5 mice, related to Figure 1.

(A) Spontaneous home cage locomotor activity measured by the e-motion system is indistinguishable between wild-type (n=7) and D1miRmGluR5 mice (n=9) (Two-way ANOVA, *genotype* effect ($F_{(1,84)}$=2.8, P <0.1). Both genotypes display typical diurnal rhythmicity with higher activity levels during the night phase compared with the resting, light phase of the day. Two-way ANOVA indicates a *phase* effect ($F_{(1,84)}$=430.5, p<0.0001), and all day points are significantly different from all night points (Newman-Keuls post-hoc test, P<0.05, not indicated). (B) D1^{miR}mGluR5 mice show a faster habituation to novelty in the activity boxes. During the first 30 min exposure (Exposure 1), both genotypes display decreased locomotor activation in the last 5 min compared to the first 5 min, indicating habituation to novelty (Two-way ANOVA, *time* effect: $F_{(9,126)}$=13, P <0.0001). However, this effect is more pronounced in D1^{miR}mGluR5 mice (*genotype* effect: $F_{(1,14)}$=10.4, P <0.01, Newman-Keuls post-hoc test indicates P <0.005 in wild-types and P <0.0001 in D1^{miR}mGluR5 mice comparing the first and the last 5 min of the exposure). After repeated exposures (Exposure 5) habituation processes are not different anymore between genotypes (Two-way ANOVA, *genotype* effect: $F_{(1,14)}$=1.6, P =0.2; *time* effect: $F_{(9,126)}$=37.3, P <0.0001; Newman-Keuls post-hoc test P <0.0001 for both genotypes comparing the first and the last 5 min of the exposure). (C-H) Anxiety-related behavior is not different between both genotypes. (C, D) Elevated plus-maze test. The time spent (C) and number of visits to the open arms (D) of the maze is almost identical in both genotypes ($t_{(51)}$=0.5, P=0.6). (E,F) similarly, in light-dark box, time spent in the light area (E) or the latency to enter the light

zone (F) is not different between wild-type and D1^{miR}mGluR5 mice ($t_{(53)} = -0.1$; P=0.9 and $t_{(53)} = 0.7$; P =0.5, respectively). (G, H) Novelty-induced grooming duration (G) and frequency (H) is indistinguishable between wild-type and D1miRmGluR5 mice ($t_{(15)} = 0.1$; P =0.9 and $t_{(15)} = 0.2$; P =0.8, respectively). (I, J) Evaluation of the short-term memory in the Y-maze test shows an intact performance in D1^{miR}mGluR5 mice, as indicated by the decreased time (I) and number of visits (J) displayed to the new arm 30 min after the first exposure (inter-trial-interval 30) (Two-way ANOVA, *inter-trial interval* effect: $F_{(1,30)} = 56$; P <0.0001 and $F_{(1,30)} = 82.6$; P <0.0001 for I&J, respectively). Data represent mean $\pm$ SEM. Two-way ANOVA, * P <0.005 and ** P <0.0001 compared with first 5 minutes; + P <0.005 compared with 2 min inter-trial interval.

Supplemental Figure 5

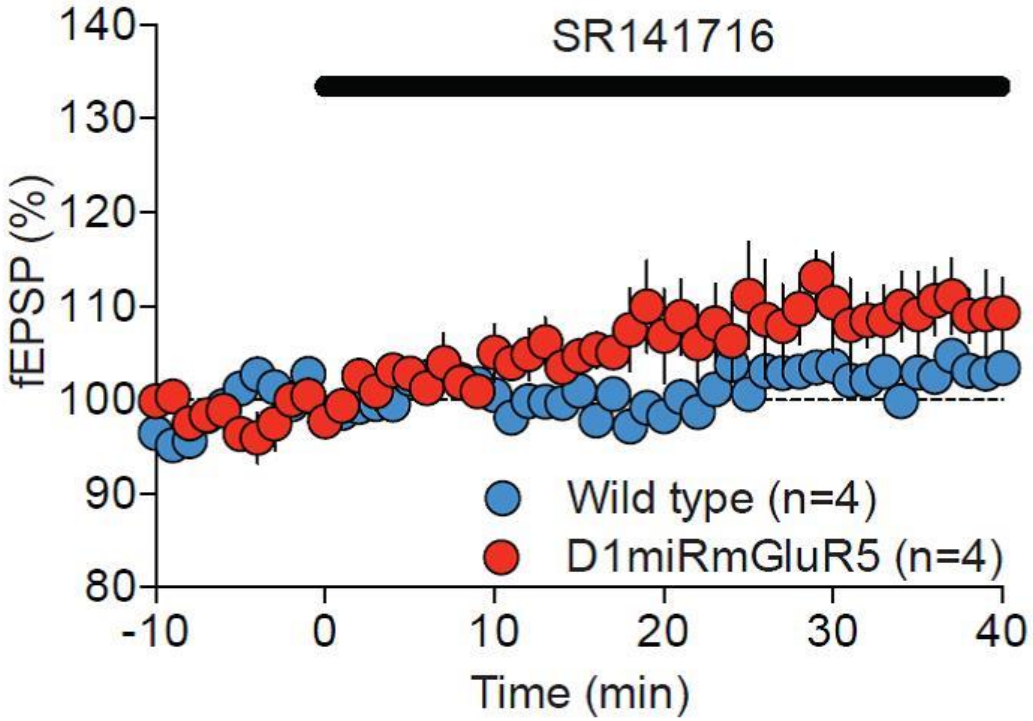

Figure S5. Tonic CB1R activation is minimal in both wild-type and D1^{miR}mGluR5 mice, related to Figure 3.

The cannabinoid inverse agonist SR141716A had no effect on baseline transmission in wild-type (blue) or D1^{miR}mGluR5 (red) mice. Average time course of mean EPSCs is represented as percentage of the basal value. All data represent mean ± SEM. Two-way ANOVA, *P < 0.05 vs. D1^{miR}mGluR5 mice.

Supplemental Figure 6

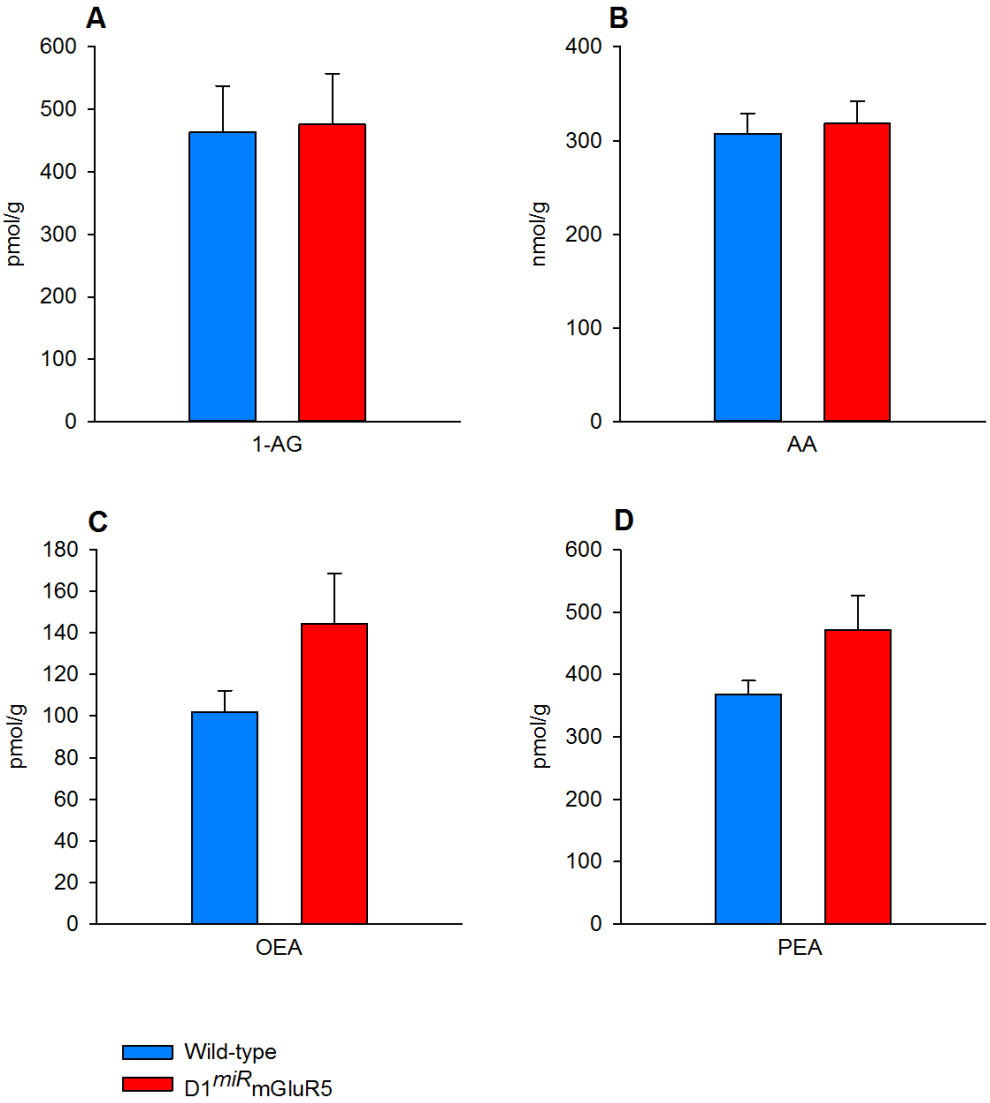

Figure S6. Basal eCB and congeners concentrations in the NAc of wild-type and D1^{miR}mGluR5 mice, related to Figure 3.

1-arachidonoyl glycerol (1-AG, (A)), arachidonic acid (AA, (B)), oleoylethanolamide (OEA, (C)) and palmitoylethanolamide (PEA, (D)) levels in NAc of wild-type (n=10) and D1^{miR}mGluR5 mice (n=10). Under basal, non-stimulated conditions, eCB and congeners levels are similar in both genotypes (Student's *t*-test, 1-AG: $t_{(18)}$=-0.1, P =0.9; AA: $t_{(18)}$= -0.3, P =0.7; OEA: $t_{(18)}$=-1.7, P =0.1; PEA: $t_{(18)}$= -1.8, P =0.1). Data represent picomoles or nanomoles/gram wet tissue ± SEM.

Supplemental Figure 7

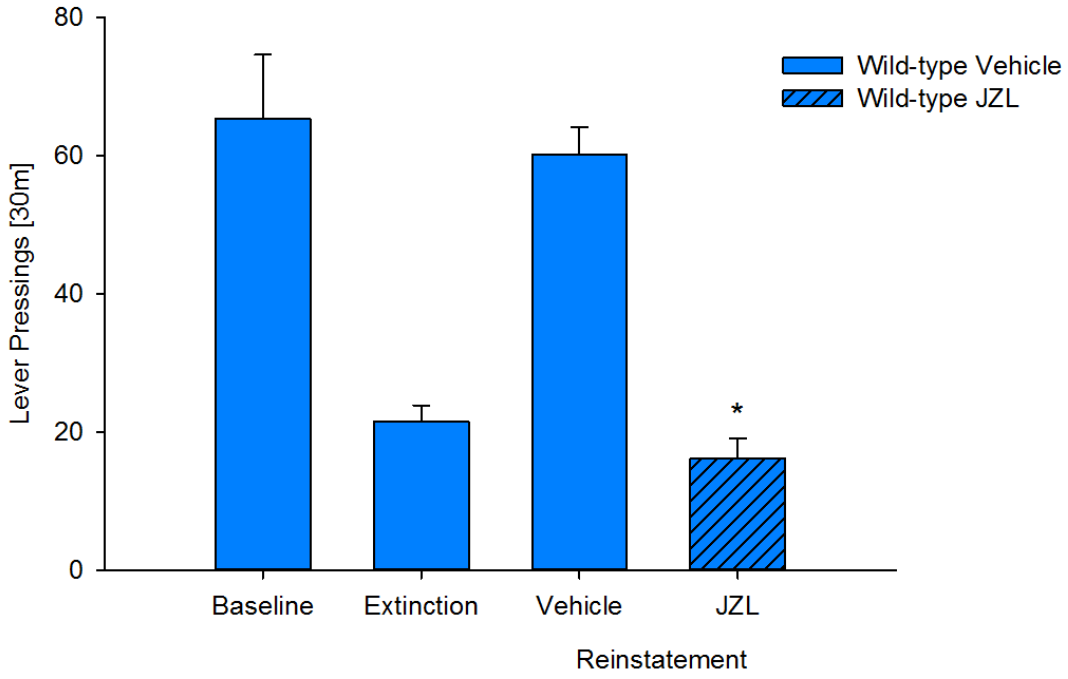

Figure S7. Effect of JZL administration on saccharin seeking behavior in wild-type mice, related to Figure 4.

In wild type mice (n=14), administration of JZL (16 mg/kg, i.p.) attenuated cue-induced reinstatement of saccharin-seeking behavior ($t_{(13)}$=9.2, P<0.0001). All data represent mean ± SEM. Student's *t*-test, **P* < 0.001 vs. vehicle treatment.

Transparent Methods

Procedures for this study complied with the regulations covering animal experimentation within the European Union (European Communities Council Directive 86/609/EEC) and Germany (Deutsches Tierschutzgesetz) and the experiment was approved by the German animal welfare authorities (Regierungspräsidium Karlsruhe).

Animals

D1^{miR}mGluR5 and wild-type male mice (6-8 weeks at the beginning of the experiments) were generated, genotyped and bred at the Central Institute of Mental Health in Mannheim. Short hairpin RNAs were designed using the sFold (sTarMir) and BLOCK-IT RNAi Designer (Invitrogen) software packages and tested in cell culture for knock-down (KD) efficiency of mGluR5 mRNA. BLOCK-iT Pol II miR RNAi Expression vector kit with GW/EmGFP-miR vector (Invitrogen) was used to insert synthetic oligos to artificial miRNA context. The construct was recombined into a bacterial artificial chromosome (BAC; RP24–179E13; Children's Hospital Oakland Research Institute, Oakland, CA) harboring the mouse D1R gene. The BAC was purified, the vector sequences were removed, and the transgene was injected into the pronuclei of fertilized oocytes from C57BL/6N mice. Experimental animals were generated by backcrossing of D1^{miR}mGluR5 transgenic mice to C57BL/6N line. Transgenic animals were genotyped using the following primers: ACGTAAACGGCCACAAGTTC, AAGTCGTGCTGCTTCATGTG (Novak et al., 2010). All animals were singly housed in standard hanging cages at 21 ± 1°C and 50 ± 5% relative humidity on a 12 h light/dark cycle, with lights on at 7:00 A.M. Animals were provided with standard rodent food and tap water *ad libitum*. Animals were handled on a daily basis before starting the experiments. Experiments were conducted in accordance with European Union guidelines on the care and use of laboratory animals.

Behavioral experiments

D1^{miR}mGluR5 and wild-type mice were tested for basic phenotype, cue-induced reinstatement of ethanol, saccharin or sucrose operant self-administration, and intracranial self-stimulation (ICSS). All experiments were performed during the active, dark phase of the day, between 9:00 and 14:00 h.

Basic Phenotype.

Characterization of locomotor, anxiety and short-term memory. The tests performed were home cage activity, habituation to the activity box, elevated plus maze paradigm, light-dark box, novelty-induced grooming and the free-choice exploration paradigm in Y-maze. All tests were performed by trained observers blind for genotypes. Devices used for all behavioral studies were carefully cleaned with a diluted acetic acid solution between animals to prevent olfactory cues.

Home cage activity. Locomotor activity in the home cage was monitored by connecting an infrared sensor (Mouse-E-Motion; Infra-E-Motion GmbH, Henstedt-Ulzburg, Germany). A Mouse-E-Motion device was placed above each cage (30 cm from the bottom), so that the mouse could be detected at any position inside the cage. The device was sampling every 4 s whether the mouse moved or not. The sensor could detect body movements of the mouse of ≥1.5 cm from one sample point to the next. Monitoring of locomotor activity started before the beginning of the experiments and lasted for 4–5 days, and data were collected every 4 h to measure the circadian pattern of motor activation.

Habituation to the activity box. This test was used to assess animal exploratory activity and reactivity to novel environment and to evaluate the effects of habituation mechanisms. Animals were placed in activity chambers in which locomotor activity was measured every min for a period of 30 min under novelty and familiarity (4 consecutive more days) conditions. Clear Plexiglas boxes of 40 cm in diameter and 40 cm in height were used, and the

locomotor activity was measured with a TruScan activity monitoring system (Coulbourn Instruments, Allentown, PA, USA).

Elevated plus maze. The plus maze consisted of 2 open arms and 2 enclosed arms extending from a central platform. The maze was elevated 50 cm above and illuminated from the top at 60 lux. Each mouse was placed at the intersection of the 4 arms of the maze and allowed to explore all 4 arms freely for 5 min, and the behavior was recorded and measured by the Noldus/EthoVision 3.1 monitoring system Wageningen, The Netherlands).

Light-dark box. The light-dark box test consisted of black and white plexiglass (45×20×27 cm) box. The dark compartment (15×27 cm) was cover and the light compartment (30×27 cm) remained open, and was kept at a luminosity of 350 lux. A door was located in the wall between the two chambers allowing free access between the light and dark compartments. Each mouse was placed in the dark chamber and was allowed to explore the box for 5 minutes, and the behavior was recorded and measured by the Noldus/EthoVision 3.1 monitoring system (Wageningen, The Netherlands).

Novelty-induced grooming. We selected novelty-induced grooming, as it represents a characteristic behavior associated with selective stimulation of D1 receptors. Mice were handled and placed in a glass observation box of 30x40x30 cm. and the time spent grooming and the number of oral stereotypies was video tracked over 10 min.

Free-choice exploration paradigm in Y-maze. This test studies working and short-term memory based in a simple measurement of novelty recognition. The test is based on the rodent's innate curiosity to explore novel areas, and it is not biased by incentives/reinforcers such as food, etc. This test was used to assess preference and/or habituation to novelty and spatial memory. The apparatus consisted of three arms of black plastic forming a "Y." Mice were placed into one of the arms of the maze (start arm) and allowed to explore only another arm of the maze for 5 min. Two min and 30 min after the first exploration interval, mice were returned to the start arm and allowed to explore freely all three arms of the Y-maze for 5 min.

The number of entries into and the time spent in each arm was recorded and measured by the Noldus/EthoVision 3.1 monitoring system (Wageningen, The Netherlands).

Operant self-administration, extinction and cue-induced reinstatement of ethanol and saccharin seeking.

Mice were trained and tested in eight operant chambers (TSE Systems, Bad Homburg, Germany), operated with operant behavior system (TSE Systems). Each chamber had two ultrasensitive levers (required force, ≤1 g) on opposite sides: one functioning as the actuve and one as the inactive lever. Next to each lever, a front panel containing the visual stimulus was installed above a drinking microreservoir. When the programmed ratio requirements were met on the active lever, 10 μl of the solution were delivered into a microreservoir, and the visual stimulus was presented via a light located on the front panel. Responses on the inactive lever were recorded but had no programmed consequences. A microcomputer controlled the delivery of fluids, presentation of auditory and visual stimuli, and recording of the behavioral data.

Conditioning phase. Mice were trained to self-administer 10% ethanol (v/v), 0.2% saccharin (w/v) or 3% sucrose (w/v) in 30 min daily sessions on a fixed ratio 1 schedule of reinforcement, where each response resulted in delivery of 10 μl of fluid. A contextual stimulus predicting reward availability was presented during the self-administration sessions. The contextual stimulus consisted of a gray, smooth floor (S^+). In addition, each lever press resulting in delivery of fluid was paired with the illumination of the chamber's cue light for 5 s (CS^+). Concurrently with the presentation of these stimuli, a 5 s time-out period was in effect, during which responses were recorded but not reinforced. Criteria for the conditioning were met at stable baseline lever pressing for 3 consecutive days, with no significant differences in lever pressing.

Extinction phase. After the last conditioning day, mice were subjected to 30-min extinction sessions. Responses at the lever activated the delivery mechanism but did not result in the

delivery of liquids or the presentation of the response-contingent cue (light). The criteria for extinction were established at 40% of the baseline lever responses for 3 consecutive days.

Reinstatement testing. Reinstatement tests began the day after the last extinction session and lasted 30 min. In ethanol, saccharin or sucrose-trained mice, cue-induced reinstatement was tested under conditions identical to those during the conditioning phase, except that the fluid was not made available.

Intracranial self-stimulation.

Mice were anesthetized with 1.5-1.8% of isoflurane (CP-Pharma, Burgdorf, Germany), stereotaxically implanted with insulated monopolar stainless steel electrodes (28 mm diameter) (Plastics One, USA) to the right medial forebrain bundle in the lateral hypothalamus (coordinates from Bregma: anterior (AP) -1.2, lateral (ML) +1, ventral (DV) −5.4), and trained to respond for brain stimulation reward (BSR).

During each testing session, mice responded during three consecutive series of 15 descending frequencies (.05 log10 steps). Maximum control rate (MCR), and total number of stimulations were calculated from the average of the second and third series. Stimulation seeking and extinction components were calculated from the total number of stimulations during the first 5 highest frequencies and the remaining 10, respectively.

Surgery and intra-NAc microinfusions.

Mice were anesthetized with 1.5-1.8% of isoflurane (CP-Pharma, Burgdorf, Germany). Unilateral cannulae were implanted under stereotaxic guidance (David Kopf Instruments, Tujunga, USA) aimed at the nucleus accumbens core (from Bregma: anterior (AP) +1.65, lateral (ML) ±0.9, ventral (DV) −4.2). Stainless steel cannulae (-4.2 mm, 26 gauge) were used. Cannulae were secured with cement (Super-Bond C&B, Sun Medical, Moriyama, Japan), and a 33-gauge stainless steel stylets were inserted into the length of each guide cannula prevent blockade and contamination. Cannulae were implanted at the end of the self-

administration training phase, and mice had 3-4 days of recovery. For microinfusions, mice were gently restrained, stylets were removed and injectors (33-gauge stainless steel tubing) were lowered 0.1mm beyond the tip of the guide cannula into the accumbens core and were attached via polyethylene tubing (PE20) to 10 µl Hamilton syringes. Infusions of 0.5 µl were delivered by a syringe pump (Harvard Apparatus, Holliston, USA) and were given over 2min (flow rate 0.25µl/min) to limit injection spread into neighboring brain areas, as well as to minimize diffusion up the injector track. To ensure complete diffusion, injectors were removed 1min after completion of the infusion.

Drugs

For the behavioral experiments, ethanol dilution (10% w/v) was made up with 95% ethyl alcohol and water. Sodium saccharin (Sigma Chemical Co., Germany) or sucrose were added to water to achieve 0.2% and 3% (w/v), respectively. Systemic, intraperitoneal treatments included AM251 (0.3 mg/kg), MTEP (20 mg/kg), JZL184 (16 mg/kg, Sigma Chemical Co., Germany) and CP55, 940 (20 µg/kg) suspended with 2–3 drops of Tween 80 in saline as vehicle and cocaine (20 mg/kg) dissolved in saline. AM251 (1µg/0.5µl), JZL (1.6 and 3µg/0.5µl) were dissolved in water administered in the NAc core.

Drugs were administered 40min (MTEP, AM251 and JZL184, i.p.), 24h (cocaine and CP55, 940, i.p.) or 1h (AM251 and JZL184, intra-accumbal) before the reinstatement, self-administration tests or in the homecage. For the operant tests, drug administrations were conducted every third day using a counterbalanced design.

Statistical analyses

Statistical analyses were performed by ANOVA with Newman-Keuls test for post-hoc comparisons, Mann Whitney U-test or Student's *t*-test. Significance was set at $P<0.05$.

Electrophysiological Experiments

Slice preparation

Nucleus accumbens (NAc) slices were prepared as follows. Briefly, mice were anesthetized with isoflurane and decapitated. The brain was sliced (300 μm) in the coronal plane (Integraslice, Campden Instruments, Leicester, U.K.) and maintained in artificial cerebrospinal fluid (ACSF) containing 126 mM NaCl, 2.5 mM KCl, 2.4 mM $MgCl_2$, 1.2 mM $CaCl_2$, 18 mM $NaHCO_3$, 1.2 mM NaH_2PO_4 and 11 mM glucose, equilibrated with 95% O_2/5% CO_2 at 4°C. Slices were then stored for 30 min at 32–35°C and at 22 ± 2 °C until recording in ACSF.

Electrophysiology

Whole-cell patch-clamp and extracellular field recordings were made from medium spiny neurons respectively, in coronal slices of mouse NAc (Deroche et al., 2020). For recording, slices were superfused (2ml/min) with ACSF. All experiments were done at 32–35 °C. The ACSF contained picrotoxin (100 μM) to block GABA-A receptors. To evoke synaptic currents, 150-200 μs stimuli were delivered at 0.1Hz through an ACSF-filled glass electrode placed at a distance > 150 μm in the dorsomedial direction (ventral striatum recordings). For extracellular field experiments, the recording pipette was filled with ACSF. The glutamatergic nature of the field excitatory postsynaptic potential (fEPSP) was confirmed at the end of each experiments using the ionotropic glutamate receptor antagonist 6, 7-dinitroquinoxaline-2,3-dione (DNQX, 20 μM), that specifically blocked the synaptic component without altering the non-synaptic component (data not shown). LTD was induced by low frequency stimulation of 10 minutes at 10 Hz. For whole-cell patch-clamp, pyramidal neurons in PFC layer V/VI and medium spiny neurons of NAc were visualized using an infrared microscope (BX-50WI or BX-51WI, Olympus). Experiments were made with electrodes containing 128mM potassium

gluconate (KGlu), 20mM NaCl, 1mM $MgCl_2$, 1mM EGTA, 0.3mM $CaCl_2$, 2mM Na^{2+}-ATP, 0.3mM Na^{+}-GTP, 10mM glucose buffered with 10mM HEPES, pH 7.3, osmolarity 290mOsm. Electrode resistance was 4–6MOhm. If access resistance (no compensation, <25MOhm) changed by >20%, the experiment was rejected. To perform the voltage-clamp experiments, evoked EPSCs were recorded at -70mV.

Retrograde tracing

Under general ketamine-xylazine anesthesia and stereotactic control, 80 nl of red or green fluorescent latex microspheres (Lumafluor, Naples, F) were pressure injected bilaterally in the ventral mesencephalon (bregma: -3.3mm, lateral: 0.6mm, ventral:4.8mm) or Ventral pallidum (bregma:0.15mm, lateral:1.8mm ventral:4.8mm). Animals were sacrificed 14-28 days after injections and brain slices prepared for electrophysiology.

Retrogradely labeled direct and indirect pathway MSNs were visualized by infrared-differential interference contrast (IR-DIC) and epifluorescence microscopy (Olympus BX-51WI).

Data acquisition and analysis

The potential reference of the amplifier was adjusted to zero before breaking into the cell or entering the slice. Data were recorded on a MultiClamp 700B or Axopatch 200B (Axon Instruments), filtered at 2kHz, digitized (20kHz, DigiData 1440A or 1322A, Axon Instrument), collected using Clampex 10.2 and analyzed using Clampfit 10.2 (all from Molecular Device, Sunnyvale, USA). Analysis of both area and amplitude of fEPSP and EPSCs was performed (graphs depict amplitudes for patch clamp experiments and areas for field recordings). The magnitude of LTD was calculated 25-30 minutes after tetanic protocol as percentage of baseline responses.

The fitting of concentration response curves was calculated according to y={ymax2ymin/1+(x/EC50)n}+ymin (where ymax=response in the absence of agonist, ymin=response remaining in presence of maximal agonist concentration, x=concentration, EC50=concentration of agonist producing 50% of the maximal response and n=slope) with GraphPad Prism 5.0 (GraphPad Software Inc., La Jolla, CA).

Drugs

Drugs were added at the final concentration to the ACSF. Picrotoxin was from Sigma (St. Quentin Fallavier, France). DNQX was from the National Institute of Mental Health's Chemical Synthesis and Drug Supply Program (Rockville, MD, USA). LY379268, JZL184 and CP55, 940 were from Tocris (Bristol, UK).

Statistical analysis

The value *n* corresponds to the number of animals. All values are given as mean ± SEM. and statistical significance was set at $P < 0.05$. Statistical analysis (ANOVA or Mann Whitney U-test), was performed with GraphPad Prism 5.0 (GraphPad Software Inc., La Jolla, CA).

Immunohistochemistry for electron microscopy

Preembedding immunocytochemical method for electron microscopy. Animals were deeply anesthetized by i.p. injection of a mixture of Nembutal (5mg/100g body weight; Abbott Laboratories Inc., IL, USA) and urethane (130mg/100g body weight; Sigma-Aldrich, St. Louis, MO, USA). They were transcardially perfused with PBS (0.1 M, pH 7.4) and then fixed with 250 ml of 4% formaldehyde, 0.1% glutaraldehyde and 0.2% saturated picric acid in PB (0.1M, pH 7.4). Perfusates were used at 4^{o}C. Tissue blocks were extensively rinsed in 0.1 M PBS (pH 7.4). Coronal brain vibrosections were cut at 50 µm and collected in 0.1 M PBS (pH 7.4) at RT. Sections containing the nucleus accumbens were preincubated in a blocking

solution of 10% bovine serum albumin (BSA), 0.1% sodium azide and 0.02% saponin prepared in Tris-HCl buffered saline (TBS, pH 7.4) for 30 minutes at RT. A preembedding silver-intensified immunogold method was used for the localization of CB1R, DAGL-α and MAGL proteins. The primary polyclonal antibodies used in this study were: polyclonal goat antibody to CB1R (2µg/ml; CB1R-Go-Af450-1; Frontier Science Co. Ltd; 1-777-12, Shinko-nishi, Ishikari, Hokkaido, Japan), polyclonal goat antibody to DAGL-α (2µg/ml; DAGL-α-Go-Af1080-1; Frontier Science Co. Ltd; 1-777-12, Shinko-nishi, Ishikari, Hokkaido, Japan) and polyclonal rabbit antibody to MAGL (1:100; Cayman Chemical Company, Michigan 48108, USA). Accumbens sections were incubated with the primary antibodies in 10% BSA/TBS containing 0.1% sodium azide and 0.004% saponin on a shaker for 1 day at RT. After several washes in 1% BSA/TBS, tissue sections were incubated in the secondary 1.4 nm gold-labeled rabbit anti-goat IgG and goat anti-rabbit IgG (Fab' fragment, 1:100, Nanoprobes Inc., Yaphank, NY, USA), depending on the primary antibodies, in 1% BSA/TBS with 0.004% saponin on a shaker for 4 hours at RT. Thereafter, the tissue was washed in 1% BSA/TBS overnight at 4ºC and postfixed in 1% glutaraldehyde in TBS for 10 minutes at RT. Following washes in double-distilled water, gold particles were silver-intensified with a HQ Silver kit (Nanoprobes Inc., Yaphank, NY, USA) for about 12 minutes in the dark and then washed in 0.1X PBS (pH 7.4). Stained sections were osmicated (1% OsO4 in 0.1X PBS, pH 7.4, 20 minutes), dehydrated in graded alcohols to propylene oxide and plastic-embedded flat in Epon 812. 80nm ultrathin sections were collected on mesh nickel grids, stained with uranyl acetate and lead citrate, and examined in a Philips EM2008S electron microscope. Tissue preparations were photographed by using a digital camera coupled to the electron microscope. Figure compositions were scanned at 500 dots per inch (dpi). Labeling and minor adjustments in contrast and brightness were made using Adobe Photoshop (CS, Adobe Systems, San Jose, CA, USA).

Analysis of the proportion of immunolabeled profiles in nucleus accumbens. Sections with nucleus accumbens processed for the localization of CB1R, DAGL-α and MAGL with preembedding immunocytochemistry were used for semi quantitative analysis. Tissue showing good and reproducible silver-intensified gold particles were cut at 80 nm. Electron micrographs (10,000-25,000X) were taken from grids (132 μm side). To avoid false negatives, only ultrathin sections in the first 1.5 μm from the surface of the tissue block were examined. Positive labelling was considered if at least one immunoparticle was over postsynaptic or presynaptic membranes, within approximately 30 nm from the membranes, or within the cellular profile in case of MAGL. Percentages of immunopositive profiles were analyzed and displayed using a statistical software package (GraphPad Prism 4, GraphPad Software Inc, San Diego, USA).

Measurement of endocannabinoid levels by LC-MS/MS analysis

Standards for endocannabinoid measurements (anandamide (AEA), 2-arachidonoyl glycerol (2-AG), 1-arachidonoyl glycerol (1-AG), oleoylethanolamide (OEA), palmitoylethanolamide (PEA), arachidonic acid (AA), and their deuterated analogues AEA-d_4, 2-AG-d_5, 1-AG-d_5, OEA-d_2, PEA-d_4, and AA-d_8) were obtained from Cayman Chemicals (Ann Arbor, Michigan, USA). Water (H_2O), acetonitrile (ACN), formic acid (FA), ethylacetate and hexane (all of Fluka LC-MS grade) were obtained from Sigma-Aldrich (Munich, Germany) and Carl Roth (Karlsruhe, Germany). All stock solutions, intermediate dilutions and calibration standards were made up with ACN at appropriate concentration levels. For the measurement of endocannabinoid levels, punches were kept frozen at -80^{o}C. Samples were weighed in the extraction tubes, spiked with acetonitrile (ACN) containing the internal standards, homogenized in ice-cold 0,1 M formic acid using the TissueLyser II (Qiagen, Hilden, Germany) and extracted with ethylacetate/hexane (9:1, v/v). The tubes were vortexed for 30 seconds, and centrifuged for 10 min at 10000 g and 4°C. The upper (organic) phase was

removed, evaporated to dryness under a gentle stream of nitrogen at 37°C and re-dissolved in ACN/H_2O (1:1, v/v). The LC-MS/MS analysis was then performed on a LC-MS/MS system consisting of a 5500 QTrap triple-quadrupole linear ion trap mass spectrometer equipped with a Turbo V Ion Source (AB SCIEX, Darmstadt, Germany) with a "positive-negative switching" mode, an Agilent 1200 series LC system (degasser, pump, and thermostated column compartment; Agilent, Waldbronn, Germany), and a CTC HTC PAL autosampler (CTC Analytics AG, Zwingen, Switzerland). ECBs and related compounds were separated on a Phenomenex Luna 2.5 µm C18(2)-HST column combined with a SecurityGuard pre-column (Phenomenex, Aschaffenburg, Germany) with solvents A: 0.1% FA in 20:80 ACN/water (v/v), and B: 0.1% FA in ACN, using the following gradient: linear from 55-90% B (0-2 min), then held at 90% B (2-7.5 min), and re-equilibrated at 55% B (7.5-10 min). The column temperature was 25°C, the LC flow rate 0.3 ml/min, and the injection volume 20 µL. Positive and negative ions were analyzed simultaneously by combining two experiments in 'positive-negative-switching' mode. The Turbo V Ion Source was operated with the electrospray ('TurboIon') probe with nitrogen as curtain and nebulizer gas, and using the following settings: Temperature 550°C, curtain gas 40 psi, GS1 50 psi, GS2 50 psi, capillary voltage -4500 V (negative) and +5500 V (positive). The following precursor-to-product ion transitions were used for multiple-reaction monitoring (MRM): positive: AEA m/z 348.3 -> 62.1, AEA-d_4 m/z 352.3 -> 66.1, 2-AG/1-AG m/z 379.1 -> 287.2, 2-AG-d_5/1-AG-d_5 m/z 384.2 -> 287.2, OEA m/z 326.2 -> 62.1, OEA-d_2 m/z 328.2 -> 62.1, PEA m/z 300.2 -> 62.1, PEA-d_4 m/z 304.2 -> 62.1; negative: AA m/z 303.1 -> 259.1, AA-d_8 311.0 -> 267.0. Data acquisition and analysis were performed using Analyst software (version 1.5.1; AB SCIEX).

Supplemental References

Deroche, M.A., Lassalle, O., Castell, L., Valjent, E., Manzoni, O.J. (2020). Cell-type and endocannabinoid specific synapse connectivity in the adult nucleus accumbens core. J Neurosci. 40(5), 1028-1041. Epub 2019 Dec 12.

Novak, M., Halbout, B., O'Connor, E.C., Rodriguez Parkitna, J., Su, T., Chai, M., Crombag, H.S., Bilbao, A., Spanagel, R., Stephens, D.N., Schütz, G., and Engblom, D. (2010). Incentive learning underlying cocaine-seeking requires mGluR5 receptors located on dopamine D1 receptor-expressing neurons. J. Neurosci. 30, 11973-11982.